NATIONAL ADVISORY COMMITTEE FOR AERONAUTICS

TECHNICAL NOTE

No. 1581

APPROXIMATE RELATIONS AND CHARTS FOR LOW-SPEED STABILITY DERIVATIVES OF SWEPT WINGS

By Thomas A. Toll and M. J. Queijo

Langley Memorial Aeronautical Laboratory
Langley Field, Va.

Washington
May 1948

E R R A T A

NACA TN No. 1581

APPROXIMATE RELATIONS AND CHARTS FOR LOW-SPEED STABILITY DERIVATIVES OF SWEPT WINGS

By Thomas A. Toll and M. J. Queijo

May 1948

Page 15, equation at bottom of page: The second term within the parentheses should be $-\frac{2\,\Delta c_{l_L}}{\pi A \cos \Lambda}$.

Page 19: Equations (34) and (35) should be replaced by the following:

$$c_{2_L} = \frac{C_L^2}{\pi A \cos \Lambda}\left(1 + \frac{A + 8\cos\Lambda}{A + 4\cos\Lambda}\,\beta' \tan\Lambda\right)\left(\frac{V'_L}{V}\right)^2 \qquad (34)$$

$$c_{2_R} = \frac{C_L^2}{\pi A \cos \Lambda}\left(1 - \frac{A + 8\cos\Lambda}{A + 4\cos\Lambda}\,\beta' \tan\Lambda\right)\left(\frac{V'_R}{V}\right)^2 \qquad (35)$$

Page 20, line 5: The sign of the second term within the brace should be +; that is

$$\ldots\left\{4\,\frac{y}{b/2} + 2\,\frac{A + 2\cos\Lambda}{A + 4\cos\Lambda}\tan\Lambda \ldots\right\}$$

Page 22, second line of equation at top of page: The first term within the brackets should be

$$\left[4\left(\frac{\bar{x}}{c}\right)^2 \frac{\tan^2\Lambda}{A^2} + \ldots\right]$$

NACA - Langley Field, Va.

NATIONAL ADVISORY COMMITTEE FOR AERONAUTICS

TECHNICAL NOTE 1581

APPROXIMATE RELATIONS AND CHARTS FOR LOW-SPEED STABILITY DERIVATIVES OF SWEPT WINGS

By Thomas A. Toll and M. J. Queijo

SUMMARY

A simplified theory has been used to derive approximate relations for the low-speed stability derivatives of swept wings. The analysis is made only for wings without dihedral, but the effects of sweep angle, aspect ratio, center-of-gravity location, and, in most instances, taper ratio are considered. Several of the relations consist of a correction factor (to account for the effects of sweep) and the derivative for an unswept wing having the same aspect ratio and taper ratio as the swept wing. Methods of extending or of extrapolating known derivatives for unswept wings to low aspect ratios are given in an appendix. In some instances, as in the case of derivatives that exist only for swept wings, the simplified theory is used to determine the absolute magnitudes of the derivatives.

The approximate relations have been used to construct charts for the stability derivatives of wings having a taper ratio of 1.0.

Calculated values for the derivatives are compared with experimental values. The comparison indicates that the calculated values are fairly reliable over a range of lift coefficient (starting from zero) that decreases as the sweep angle increases. Large discrepancies between calculated and experimental values are found for highly swept wings at the high lift coefficients for which the flow is believed to be partially separated from the wing surfaces. Even a more rigorous method, if based on potential-flow concepts, probably would not provide much improvement in the range of lift coefficient for which partial separation exists.

INTRODUCTION

Rigorous solutions for the low-speed characteristics of swept wings are, at present, so cumbersome that a number of the stability derivatives have not yet been investigated. Estimates of some of the derivatives frequently have been made, however, by means of an approximate theory such as that proposed by Betz (reference 1). Although results obtained by such methods are rough approximations, the use of more precise methods frequently is not justified because of the amount of work involved and because of certain basic limitations of even the most rigorous methods.

The application of a simple theory is extremely convenient since equations can be derived to indicate the effects of individual geometric parameters, such as sweep or aspect ratio. For the more rigorous methods known, the effects of a single geometric parameter can be determined only by making separate solutions for different plan forms in order to cover an adequate range of values of the parameter being investigated.

Some confusion has resulted in the past because different interpretations have been given to the simple theory, and consequently, varying results have been obtained. In the present paper, equations for the stability derivatives of swept wings are derived from a particular application of simple sweep theory. The method used accounts approximately for the effects of the induced angle of attack, which generally has been neglected in previous applications of simple sweep theory, but neglects any effects of sweep on the load distribution.

SYMBOLS

The symbols used in the analysis and in the presentation of the results are defined herein. All spans and chords are measured perpendicular and parallel, respectively, to the plane of symmetry. Angles of attack are measured in the plane of symmetry, unless specified differently.

p,q,r angular velocities about X-, Y-, and Z-axes, respectively (see fig. 1)

c_l section lift coefficient $\left(\frac{\text{Airfoil section lift}}{\frac{1}{2}\rho V^2 c}\right)$

C_L lift coefficient $\left(\frac{\text{Lift}}{\frac{1}{2}\rho V^2 S}\right)$

C_D drag coefficient $\left(\frac{\text{Drag}}{\frac{1}{2}\rho V^2 S}\right)$

C_Y lateral-force coefficient $\left(\frac{\text{Lateral force}}{\frac{1}{2}\rho V^2 S}\right)$

C_m pitching-moment coefficient $\left(\frac{\text{Pitching moment}}{\frac{1}{2}\rho V^2 S\bar{c}}\right)$

C_l rolling-moment coefficient $\left(\frac{\text{Rolling moment}}{\frac{1}{2}\rho V^2 Sb}\right)$

C_n yawing-moment coefficient $\left(\frac{\text{Yawing moment}}{\frac{1}{2}\rho V^2 Sb}\right)$

C_l primary force coefficient $\left(\frac{F_l}{\frac{1}{2}\rho V^2 S}\right)$

F_l component of resultant semispan load directed normal to plane formed by velocity vectors V and V_n (see fig. 2)

C_2 primary force coefficient $\left(\frac{F_2}{\frac{1}{2}\rho V^2 S}\right)$

F_2 component of resultant semispan load directed parallel to velocity vector V_n (see fig. 2)

c_l section primary force coefficient $\left(\frac{f_l}{\frac{1}{2}\rho V^2 c}\right)$

f_l component of resultant section load directed normal to plane formed by velocity vectors V' and V_n'

c_2 section primary force coefficient $\left(\frac{f_2}{\frac{1}{2}\rho V^2 c}\right)$

f_2 component of resultant section load directed parallel to velocity vector V_n'

ρ mass density, slugs per cubic foot

S wing area

V flight velocity

V_n component of flight velocity normal to wing quarter-chord line

V_s component of flight velocity parallel to wing quarter-chord line

V' local resultant velocity at any spanwise station

V_n' component of local resultant velocity normal to wing quarter-chord line at any spanwise station

b wing span

c wing chord

$\bar{c}$ wing mean chord (b/A)

x longitudinal distance rearward from coordinate origin (airplane center of gravity) to wing quarter-chord line at any spanwise station

x' longitudinal distance rearward from wing aerodynamic center to wing quarter-chord line at any spanwise station

$\bar{x}$	longitudinal distance rearward from coordinate origin (airplane center of gravity) to wing aerodynamic center
y	absolute value of spanwise distance from plane of symmetry to any station on wing quarter-chord line
$\bar{y}_{L'_\beta}$	effective lateral center-of-pressure location of resultant load causing rolling moment due to sideslip
$\bar{y}_{L'_p}$	effective lateral center-of-pressure location of resultant load causing rolling moment due to rolling
$\bar{y}_{N_p}$	effective lateral center-of-pressure location of resultant load causing yawing moment due to rolling
$\bar{y}_{L'_r}$	effective lateral center-of-pressure location of resultant load causing rolling moment due to yawing
$\bar{y}_{N_r}$	effective lateral center-of-pressure location of resultant load causing yawing moment due to yawing
β	angle of sideslip, radians unless specified differently
β'	local angle of sideslip; angle between plane of symmetry and local air-stream direction at quarter-chord line of any section, radians
α	angle of attack, radians unless specified differently
α_n	angle of attack, measured between plane of wing and component of velocity normal to wing quarter-chord line
$\Delta\alpha$	incremental change in angle of attack, caused by rolling, at any spanwise station
θ	angle between Z-axis and vector representing primary force coefficient C_l (or c_l)
Λ	angle of sweep or skew of wing quarter-chord line, degrees
A	aspect ratio $\left(\frac{b^2}{S}\right)$
λ	taper ratio $\left(\frac{\text{Tip chord}}{\text{Root chord}}\right)$
Γ	dihedral angle, radians
E_θ	effective edge-velocity correction factor for lift
E_θ'	effective edge-velocity correction factor for rolling moment

$\frac{pb}{2V}$ wing-tip helix angle

$\frac{rb}{2V}$ lateral flight-path curvature

$\frac{qc}{2V}$ longitudinal flight-path curvature

a_o section lift-curve slope for section normal to quarter-chord line when placed in direction of free stream

$$C_{L_\alpha} = \frac{\partial C_L}{\partial \alpha}$$

$$C_{l_\beta} = \frac{\partial C_l}{\partial \beta}$$

$$C_{Y_\beta} = \frac{\partial C_Y}{\partial \beta}$$

$$C_{n_\beta} = \frac{\partial C_n}{\partial \beta}$$

$$C_{l_p} = \frac{\partial C_l}{\partial\left(\frac{pb}{2V}\right)}$$

$$C_{Y_p} = \frac{\partial C_Y}{\partial\left(\frac{pb}{2V}\right)}$$

$$C_{n_p} = \frac{\partial C_n}{\partial\left(\frac{pb}{2V}\right)}$$

$$C_{l_r} = \frac{\partial C_l}{\partial\left(\frac{rb}{2V}\right)}$$

$$C_{Y_r} = \frac{\partial C_Y}{\partial\left(\frac{rb}{2V}\right)}$$

$$C_{n_r} = \frac{\partial C_n}{\partial\left(\frac{rb}{2V}\right)}$$

$$C_{L_q} = \frac{\partial C_L}{\partial\left(\frac{qc}{2V}\right)}$$

$$C_{m_q} = \frac{\partial C_m}{\partial\left(\frac{qc}{2V}\right)}$$

Subscripts:

L	left wing panel
R	right wing panel
i	induced
$\Lambda=0^\circ$	restricted to zero sweep
$\beta=0^\circ$	restricted to zero sideslip
o	profile
1,2,3	first, second, and third increments, respectively

ANALYSIS

Scope

Relations for the stability derivatives of swept wings are derived from an approximate theory. The derivations are considered applicable to a system of stability axes (see fig. 1), although certain approximations have been made in representing the axis system. The equations obtained are summarized in table I. Several of the relations are in terms of the derivatives for unswept wings with the same aspect ratio and taper ratio as the swept wings. It is assumed that the derivatives for unswept wings can be obtained by more exact theories or from experimental data. Since much of the available theoretical information on the derivatives of unswept wings is limited to aspect ratios greater than 6, methods of extending or of extrapolating these derivatives to lower aspect ratios are developed in an appendix. In some instances, rigorous methods are developed for extending the derivatives to zero aspect ratio. In most cases, however, techniques based on extrapolations are used, and in these cases values for the derivatives are given to an aspect ratio of 1.0. The extrapolated values become less reliable, of course, as the aspect ratio decreases.

The analysis applies only to wings without dihedral, but it includes the effects of sweep, aspect ratio, center-of-gravity location, and, in most instances, taper ratio. The method, however, is believed to become less reliable as the taper ratio departs from unity. Charts, based on the equations and values of the derivatives given in the appendix for unswept wings, are presented in figures 3 to 15 for swept wings having a taper ratio of 1.0. Some comparisons are made with experimental data.

Basic Concepts

The method consists of an application of strip theory with approximate consideration given to the effects of aerodynamic induction. Expressions are derived for the magnitudes of the components of the resultant force acting at a section of a wing under conditions of straight flight, sideslipping flight, rolling flight, yawing flight, and pitching flight. Approximate equations for the stability derivatives of constant-chord swept wings are derived from the orientation and magnitudes of the force components for a given flight condition. In the case of derivatives which exist for both swept and unswept wings, the approximate equations are used only for the determination of correction factors for the effects of sweep; these correction factors may be applied to experimental or rigorous theoretical values of the derivatives for unswept wings and are considered to be reasonably reliable for wings having taper ratios as low as 0.5. The approximate theory indicates that certain derivatives exist only for wings with sweep. Such derivatives must be evaluated directly by the approximate theory.

In order to account for induction effects, it is assumed that the familiar expression (from lifting-line theory) for the induced angle of attack of unswept elliptic wings

$$\alpha_i = \frac{C_L}{\pi A} \tag{1}$$

is also applicable to swept wings and that the same expression may be used to determine the local induced angle at any section provided the local section lift coefficient, rather than the wing lift coefficient, is substituted in equation (1). This procedure amounts to a reduction in the two-dimensional lift load by a factor that remains constant along a semispan of the wing. Although the assumption regarding the local induced angle of attack is known to be inaccurate, the consistent application of this assumption to both swept and unswept wings is expected to yield reasonably reliable correction factors for the effects of sweep. The effects of sweep on the distribution of loading are, of course, neglected in the strip-theory treatment. The present method, therefore, can be expected to account only for the geometric effects of sweep.

Certain limitations of the present simplified treatment have been observed experimentally. For example, when the sweep angle is referred to the wing quarter-chord line, the wing lift-curve slope is found to decrease somewhat more rapidly with sweepforward than with sweepback, particularly for highly tapered wings. Although such trends cannot be predicted by the present method, they probably could be accounted for to some extent if the sweep angle were referred to some wing reference line other than the quarter-chord line. In the absence of sufficient experimental data to permit the choice of a more suitable reference line, however, the use of the quarter-chord line is retained for the present analysis.

Straight Flight

The application of the method of analysis to the straight-flight condition can be illustrated by comparing the two panels of a swept wing to skewed wings with tips cut parallel to the air stream (fig. 2). According to strip theory the load distribution in straight flight is uniform across the span of a constant-chord wing and, therefore, the total load on a panel can be considered to act at a single point (the center of pressure of the panel).

The lift coefficient for an infinite wing skewed at an angle Λ is given by

$$c_l = \alpha_n a_o \cos^2 \Lambda$$

where α_n is the angle of attack measured between the velocity component normal to the wing quarter-chord line and the wing surface, and a_o is the section lift-curve slope of the wing when placed normal to the air stream. From the assumptions of lifting-line theory, the lift coefficient of a finite skewed wing is approximately

$$C_L = \left(\frac{\alpha}{\cos \Lambda} - \frac{\alpha_i}{\cos \Lambda}\right) a_o \cos^2 \Lambda \qquad (2)$$

where the angles α and α_i are measured in a vertical plane that includes the vector representing the relative wind (the wing quarter-chord line is assumed to lie in a horizontal plane with the wing at zero angle of attack). The induced angle of attack α_i for a skewed wing is given approximately by equation (1) provided A is the aspect ratio based on the wing span perpendicular to the relative wind. Substitition of equation (1) in equation (2) gives

$$C_L = \left(\alpha - \frac{C_L}{\pi A}\right) a_o \cos \Lambda$$

which reduces to

$$C_L = \frac{a_o \cos \Lambda}{1 + \frac{a_o \cos \Lambda}{\pi A}} \alpha$$

or, by substituting 2π for a_o in the denominator,

$$C_L = \frac{A a_o \cos \Lambda}{A + 2 \cos \Lambda} \alpha$$

A panel of a swept wing at an angle of attack can be represented by one-half of a skewed wing, provided the skewed wing is rotated through an angle θ (which depends on the angle of attack of the swept wing) about an axis alined with the relative wind. (See fig. 2.) The lift force, therefore, must also be rotated through the same angle, which is given by

$$\theta = \alpha \tan \Lambda$$

A coefficient representing the rotated lift-force vector for a single panel of a swept wing will be designated as the primary force coefficient C_1, which has the magnitude

$$C_1 = \frac{1}{2} \frac{Aa_o \cos \Lambda}{A + 2 \cos \Lambda} \alpha \tag{3}$$

and which is directed perpendicular to the plane formed by the velocity vectors V and V_n (fig. 2).

For a skewed wing, the induced angle of attack measured in a vertical plane that includes the vector representing the relative wind is given by equation (1). The induced angle in a plane normal to the quarter-chord line, therefore, is

$$\alpha_{n_i} = \frac{C_L}{\pi A \cos \Lambda}$$

For a swept-wing panel, therefore, a second primary force coefficient C_2 has the following magnitude:

$$C_2 = \frac{C_L^2}{2\pi A \cos \Lambda} \tag{4}$$

The force represented by this coefficient has the same direction as the component of the flow velocity normal to the quarter-chord line of the wing.

Lift-curve slope.- For small angles of attack in straight flight, the effect on the lift coefficient of the tilt of the vectors representing the primary force coefficient C_1 can be neglected; therefore, the total lift coefficient of a swept wing is simply

$$C_L = 2C_1 \tag{5}$$

By substituting equation (3) in equation (5), the lift-curve slope obtained from an adaptation of lifting-line theory is found to be given by

$$C_{L_\alpha} = \frac{Aa_o \cos \Lambda}{A + 2 \cos \Lambda} \tag{6}$$

Equation (6) is subject to the limitations of lifting-line theory which become important at low aspect ratios. A more reliable value of C_{L_α} for swept wings may be obtained if the simple theory is used to derive a correction factor (to account for the effects of sweep) which may be applied to values of C_{L_α} of unswept wings, as derived from more precise methods. For unswept wings, equation (6) reduces to

$$\left(C_{L_\alpha}\right)_{\Lambda=0^\circ} = \frac{Aa_o}{A + 2}$$

which may be used in conjunction with equation (6) to give

$$C_{L_\alpha} = \frac{(A + 2)\cos \Lambda}{A + 2 \cos \Lambda}\left(C_{L_\alpha}\right)_{\Lambda=0^\circ} \tag{7}$$

where $\left(C_{L_\alpha}\right)_{\Lambda=0^\circ}$ is the lift-curve slope of an unswept wing with the same aspect ratio and taper ratio as the swept wing. Values of $\left(C_{L_\alpha}\right)_{\Lambda=0^\circ}$ can be obtained from experiments or from an accurate theory such as that of reference 2.

If the factor $\frac{A + 2}{A + 2 \cos \Lambda}$ is omitted from equation (7), the following simple equation is obtained:

$$C_{L_\alpha} = \left(C_{L_\alpha}\right)_{\Lambda=0^\circ} \cos \Lambda \tag{8}$$

This equation, which applies strictly only at infinite aspect ratio, has been used to some extent in the past for finite aspect-ratio wings and results from a particular interpretation of the simple theory for the condition in which the effect of the induced angle is neglected.

Equation (7) can be derived to give the effects of sweeping fixed wing panels, in which case A' is the aspect ratio of the unswept wing and, at least for untapered wings, is equal to $A/\cos^2\Lambda$. The alternate equation is

$$C_{L_\alpha} = \frac{(A' + 2)\cos \Lambda}{A' + \frac{2}{\cos \Lambda}}\left(C_{L_\alpha}\right)_{A',\Lambda=0^\circ}$$

where $\left(C_{L_\alpha}\right)_{A',\Lambda=0^\circ}$ is the lift-curve slope of the unswept wing from which the swept wing was derived and A' is the aspect ratio of the unswept wing.

If the factor $\frac{A' + 2}{A' + \frac{2}{\cos \Lambda}}$ is neglected from the equation just given, another simple equation is obtained, which arises from a second interpretation of the simple theory for the condition in which the effect of the induced angle is neglected:

$$C_{L_\alpha} = \left(C_{l_\alpha}\right)_{A',\Lambda=0^\circ} \cos \Lambda \tag{9}$$

A comparison of the results calculated from equations (7), (8), and (9) with the more precise theory developed by Mutterperl (reference 3) is given in figure 3. Results obtained from equation (7) are in good agreement with Mutterperl's results; whereas, equation (8) overestimates the effects of sweep and equation (9) underestimates the effects of sweep. At aspect ratios approaching zero, results obtained either by Mutterperl's method or by equation (7) are in agreement with Jones' theory (reference 4).

Induced drag.- The induced drag of a swept wing is, to the first order,

$$C_{D_i} = 2C_2 \cos \Lambda \tag{10}$$

Substituting the expression for C_2 (equation (4)) in equation (10) gives, as a direct consequence of the basic assumption that the induced angle of attack is given by equation (1), the following equation:

$$C_{D_i} = \frac{C_L^2}{\pi A} \tag{11}$$

Equation (11) indicates that, to a first approximation, the induced drag is independent of sweep. Some effects of sweep on the induced drag would, of course, be expected because of changes in the load distribution which are not considered in the present method. Theoretical results presented in reference 3 for the induced drag of swept wings are in fair agreement with equation (11), and, therefore, some support is given to the present assumption regarding the induced angle of attack.

Sideslipping Flight

For a constant-chord swept wing in sideslip, according to strip theory the distribution of load is uniform over each panel, although the magnitude of the load on the left panel is different from that on the right panel. As in the case of straight flight, therefore, the components of the total load on each panel may be represented for convenience by vectors located at the centers of pressure of the panels.

The panel loads are altered by sideslip because of the effect of sideslip on the velocity components normal to the quarter-chord lines of the panels and on the angles of attack with respect to the normal-velocity components. The component of velocity normal to the quarter-chord line of the left wing panel of a swept wing is altered due to sideslip by the factor $\frac{\cos(\Lambda + \beta)}{\cos \Lambda}$, and the angle of attack with respect to the normal velocity component is altered by the reciprocal of the same factor. The lift on a panel of an infinite-span swept wing is proportional to the square of the normal component of velocity and to the first power of the angle of attack. The increment of lift due to sideslip for the left panel of an infinite-span wing, therefore, can be written as

$$\Delta c_{l_L} = (c_l)_{\beta=0^\circ}\left[\frac{\cos(\Lambda + \beta)}{\cos \Lambda} - 1\right]$$

Inasmuch as

$$(c_l)_{\beta=0^\circ} = \alpha a_o \cos \Lambda$$

and for small angles of sideslip $\sin \beta \approx \beta$ and $\cos \beta \approx 1$, the following equation is obtained:

$$\Delta c_{l_L} = -\beta\alpha a_o \sin \Lambda$$

The primary-force-coefficient increment, resulting from sideslip, for a finite-span wing can be written as

$$\Delta C_{l_L} = \frac{1}{2}(\Delta c_{l_L} - \text{Induced lift coefficient})$$

The lift distribution resulting from sideslip is antisymmetrical with respect to the plane of symmetry and, therefore, the aspect ratio that determines the magnitude of the induced angle of attack is one-half of the wing geometric aspect ratio. The induced angle for the left wing panel in planes parallel to the plane of symmetry can be shown to be given by the expression

$$\alpha_{i_L} = \frac{4\ \Delta C_{l_L} \cos^3 \Lambda}{\pi A \cos^3(\Lambda + \beta)}$$

Therefore

$$\Delta C_{l_L} = \frac{1}{2}\left[-\beta\alpha a_o \sin \Lambda - \frac{4\ \Delta C_{l_L} \cos^3 \Lambda}{\pi A \cos^3(\Lambda + \beta)} a_o \cos \Lambda\right]$$

With the aid of the relation between α and C_L given by equation (6),

$$\Delta C_{l_L} = - \frac{C_L}{2} \frac{A + 2 \cos \Lambda}{A + 4 \cos \Lambda} \beta \tan \Lambda$$

The total value of the primary force coefficient for the left wing panel for combined symmetrical and antisymmetrical loads is

$$C_{l_L} = \frac{C_L}{2} \left(1 - \frac{A + 2 \cos \Lambda}{A + 4 \cos \Lambda} \beta \tan \Lambda \right) \tag{12}$$

and similarly for the right wing panel

$$C_{l_R} = \frac{C_L}{2} \left(1 + \frac{A + 2 \cos \Lambda}{A + 4 \cos \Lambda} \beta \tan \Lambda \right) \tag{13}$$

For the purpose of obtaining expressions for derivatives with respect to sideslip, in which case the antisymmetrical load is small relative to the symmetrical load, the combined load, in the determination of the induced angle of attack, may be assumed to be symmetrical with respect to the plane of symmetry. The induced angle of attack in a plane perpendicular to the quarter-chord line of the left wing panel is

$$\alpha_{i_L} = \frac{2 C_{l_L} \cos^2 \Lambda}{\pi A \cos^3 (\Lambda + \beta)}$$

The coefficient of the force directed parallel to the normal component of velocity on the left wing panel, therefore, is

$$C_{2_L} = \frac{2 C_{l_L}^2 \cos^2 \Lambda}{\pi A \cos^3 (\Lambda + \beta)} \tag{14}$$

and, on the right wing panel,

$$C_{2_R} = \frac{2 C_{l_R}^2 \cos^2 \Lambda}{\pi A \cos^3 (\Lambda - \beta)} \tag{15}$$

Rolling moment.- An increment of rolling moment due to sideslip, resulting from sweep, can be expressed as

$$\Delta C_l = \left(C_{l_L} - C_{l_R} \right) \frac{\bar{y}_{L'} \beta}{b} \tag{16}$$

By combining equations (12) and (13) with equation (16), the derivative is as follows:

$$\Delta C_{l_\beta} = -\frac{C_L}{2}\frac{\bar{y}_{L'\beta}}{b/2}\frac{A + 2\cos\Lambda}{A + 4\cos\Lambda}\tan\Lambda$$

Approximate values of the center of pressure $\frac{\bar{y}_{L'\beta}}{b/2}$ are given in the appendix.

An additional increment of rolling moment due to sideslip, which is also proportional to the lift coefficient, is found to exist for unswept wings. (See appendix.) The total value of the derivative therefore can be expressed as

$$C_{l_\beta} = C_L\left[\left(\frac{\Delta C_{l_\beta}}{C_L}\right)_{\Lambda=0^\circ} - \frac{\bar{y}_{L'\beta}}{b/2}\frac{A + 2\cos\Lambda}{A + 4\cos\Lambda}\frac{\tan\Lambda}{2}\right] \tag{17}$$

Lateral force.- The approximate theory indicates a lateral force due to sideslip given by the relation

$$C_Y = \left(C_{2_L} - C_{2_R}\right)\sin\Lambda - \left(C_{l_L}\theta_L - C_{l_R}\theta_R\right)\cos\beta \tag{18}$$

where θ_L and θ_R are the angles about an axis alined with the relative wind through which the vectors C_{l_L} and C_{l_R} are rotated because of the angle of attack and the angle of sideslip. The angles θ_L and θ_R are

$$\theta_L = \alpha\frac{\sin\Lambda}{\cos(\Lambda + \beta)}$$

and

$$\theta_R = \alpha\frac{\sin\Lambda}{\cos(\Lambda - \beta)}$$

These equations for θ_L and θ_R, equations (12) to (15), and the relation between C_L and α as given by equation (6) with a_o equal to 2π show that

$$C_{2_L} - C_{2_R} = \frac{C_L{}^2\tan\Lambda}{\pi A\cos\Lambda}\frac{A + 8\cos\Lambda}{A + 4\cos\Lambda}\beta$$

and

$$C_{l_L}\theta_L - C_{l_R}\theta_R = \frac{C_L{}^2\tan^2\Lambda}{\pi A}\frac{A + 2\cos\Lambda}{A + 4\cos\Lambda}\beta$$

Substitition of these relations in equation (18) leads to

$$C_{Y_\beta} = C_L^2 \frac{6 \tan \Lambda \sin \Lambda}{\pi A(A + 4 \cos \Lambda)} \tag{19}$$

Yawing moment.- An increment of yawing moment due to sideslip, resulting from sweep, can be expressed as

$$\Delta C_n = -\left(C_{2_L} - C_{2_R}\right)\left(\frac{\cos \Lambda}{4} + \frac{\bar{x}}{b} \sin \Lambda\right) + \left(C_{l_L}\theta_L + C_{l_R}\theta_R\right)\frac{\sin \beta}{4} + \left(C_{l_L}\theta_L - C_{l_R}\theta_R\right)\frac{\bar{x}}{b} \tag{20}$$

By means of equations (12) and (13) and the expressions given for θ_L and θ_R, it can be shown that

$$C_{l_L}\theta_L + C_{l_R}\theta_R = \frac{C_L^2 \tan \Lambda}{2\pi A \cos \Lambda}(A + 2 \cos \Lambda)$$

The incremental derivative, resulting from sweep, for the yawing moment due to sideslip, therefore, is found from equation (20) to be

$$\Delta C_{n_\beta} = -C_L^2 \frac{\tan \Lambda}{\pi A(A + 4 \cos \Lambda)}\left(\cos \Lambda - \frac{A}{2} - \frac{A^2}{8 \cos \Lambda} + 6\frac{\bar{x}}{\bar{c}} \frac{\sin \Lambda}{A}\right)$$

An additional increment of yawing moment due to sideslip, which is also proportional to C_L^2, exists for unswept wings. (See appendix.) The total value of the derivative, therefore, can be expressed as

$$C_{n_\beta} = C_L^2 \left[\left(\frac{\Delta C_{n_\beta}}{C_L^2}\right)_{\Lambda=0^\circ} - \frac{\tan \Lambda}{\pi A(A + 4 \cos \Lambda)}\left(\cos \Lambda - \frac{A}{2} - \frac{A^2}{8 \cos \Lambda} + 6\frac{\bar{x}}{\bar{c}} \frac{\sin \Lambda}{A}\right)\right] \tag{21}$$

Rolling Flight

The total load on a rolling wing is made up of a symmetrical load resulting from angle of attack and an antisymmetrical load resulting from rolling velocity. As in the case of sideslipping flight, the induced angle of attack associated with the antisymmetrical load is assumed to be determined by the aspect ratio of a single wing panel; therefore, at any spanwise section on the left wing panel the section primary force coefficient is as follows:

$$\Delta c_{l_L} = \left(\frac{|\Delta \alpha|}{\cos \Lambda} - \frac{2 \Delta c_{l_L}}{\pi A \cos \Lambda}\right) a_o \cos^2 \Lambda$$

where $|\Delta\alpha|$ is the absolute value of the change in angle of attack, caused by rolling, at any section. From this definition,

$$|\Delta\alpha| = \frac{y}{b/2}\frac{pb}{2V}$$

and, therefore,

$$\Delta c_{l_L} = \frac{Aa_o \cos\Lambda}{A + \frac{2a_o \cos\Lambda}{\pi}}\frac{y}{b/2}\frac{pb}{2V}$$

or, by substituting 2π for a_o in the denominator,

$$\Delta c_{l_L} = \frac{Aa_o \cos\Lambda}{A + 4\cos\Lambda}\frac{y}{b/2}\frac{pb}{2V}$$

The total value of the section primary force coefficient for combined symmetrical and antisymmetrical loads at any section on the left wing panel is

$$c_{l_L} = C_L - \frac{Aa_o \cos\Lambda}{A + 4\cos\Lambda}\frac{y}{b/2}\frac{pb}{2V} \tag{22}$$

and, similarly, for the right wing panel

$$c_{l_R} = C_L + \frac{Aa_o \cos\Lambda}{A + 4\cos\Lambda}\frac{y}{b/2}\frac{pb}{2V} \tag{23}$$

For the purpose of calculating values of the derivatives with respect to roll, in which case the antisymmetrical load is small compared with the symmetrical load, the induced angle of attack resulting from combined symmetrical and antisymmetrical loads can be assumed to be given by the relation used to calculate the induced angle resulting from a symmetrical load. The magnitude of the induced angle, however, is determined by the actual load on the panel. Therefore,

$$c_{2_L} = \frac{c_{l_L}^2}{\pi A \cos\Lambda} \tag{24}$$

and

$$c_{2_R} = \frac{c_{l_R}^2}{\pi A \cos\Lambda} \tag{25}$$

Rolling moment.- At low angles of attack the coefficient or rolling moment due to rolling can be expressed as

$$C_l = \frac{1}{b^2}\int_0^{b/2} \left(c_{l_L} - c_{l_R}\right) y \, dy \tag{26}$$

After substitution in equation (26) of the values of c_{l_L} and c_{l_R} given by equations (22) and (23), the strip-theory value of the derivative of rolling moment due to rolling is found to be

$$C_{l_p} = -\frac{1}{6}\frac{Aa_o \cos \Lambda}{A + 4 \cos \Lambda}$$

which can be rewritten in a form similar to that of equation (7); that is,

$$C_{l_p} = \frac{(A + 4)\cos \Lambda}{A + 4 \cos \Lambda}\left(C_{l_p}\right)_{\Lambda=0^\circ} \tag{27}$$

The equation for C_{l_p} actually should contain additional terms dependent on the angle of attack and the center-of-gravity location. Such terms generally are small, however, and are therefore neglected in the present approximate treatment.

Lateral force.- The coefficient of lateral force due to rolling is given by

$$C_Y = \frac{1}{b}\int_0^{b/2} \left[\left(c_{2_L} - c_{2_R}\right)\sin \Lambda - \left(c_{l_L}\theta_L - c_{l_R}\theta_R\right)\right] dy \tag{28}$$

where

$$\theta_L = \left(\alpha - \frac{y}{b/2}\frac{pb}{2V}\right)\tan \Lambda$$

and

$$\theta_R = \left(\alpha + \frac{y}{b/2}\frac{pb}{2V}\right)\tan \Lambda$$

From equations (22) to (25) and from the approximate relation between α and C_L as given by equation (6) for a_o equal to 2π, it can be shown that

$$c_{2_L} - c_{2_R} = -\frac{8C_L}{A + 4 \cos \Lambda}\frac{y}{b/2}\frac{pb}{2V}$$

$$c_{l_L}\theta_L - c_{l_R}\theta_R = -4C_L \tan \Lambda \frac{y}{b/2}\frac{pb}{2V}\frac{A + 3 \cos \Lambda}{A + 4 \cos \Lambda}$$

After substituting these relations in equation (28) and performing the integration, the derivative of lateral force due to rolling is

$$C_{Y_p} = C_L \frac{A + \cos \Lambda}{A + 4 \cos \Lambda} \tan \Lambda \tag{29}$$

Yawing moment.- The coefficient of yawing moment due to rolling is

$$C_n = -\frac{1}{b^2} \int_0^{b/2} \left[\left(c_{l_L} + c_{l_R} \right) \frac{y}{b/2} \frac{pb}{2V} y + \left(c_{2_L} - c_{2_R} \right) \left(y \cos \Lambda + x \sin \Lambda \right) \right.$$

$$\left. - \left(c_{l_L} \theta_L - c_{l_R} \theta_R \right) x \right] dy \tag{30}$$

where

$$x = \bar{x} + \left(y - \frac{b}{4} \right) \tan \Lambda$$

and, from equations (22) and (23),

$$c_{l_L} + c_{l_R} = 2C_L$$

After substituting the appropriate expressions for $c_{l_L} - c_{l_R}$, $c_{2_L} - c_{2_R}$, $c_{l_L}\theta_L - c_{l_R}\theta_R$, and x in equation (30), the derivative of yawing moment due to rolling is found to be

$$C_{n_p} = -\frac{C_L}{6} \frac{A + 6(A + \cos \Lambda)\left(\frac{\bar{x}}{\bar{c}} \frac{\tan \Lambda}{A} + \frac{\tan^2 \Lambda}{12} \right)}{A + 4 \cos \Lambda}$$

The approximate theory is then used to obtain a correction factor for the effects of sweep to be applied to the derivative for the unswept wing, thus,

$$C_{n_p} = C_L \frac{A + 4}{A + 4 \cos \Lambda} \left[1 + 6 \left(1 + \frac{\cos \Lambda}{A} \right) \left(\frac{\bar{x}}{\bar{c}} \frac{\tan \Lambda}{A} + \frac{\tan^2 \Lambda}{12} \right) \right] \left(\frac{C_{n_p}}{C_L} \right)_{\Lambda=0^\circ} \tag{31}$$

The value of C_{n_p} depends upon the center-of-gravity location because of the existence of a lateral force due to rolling. When $\bar{x}$ is zero, equation (31) becomes

$$C_{n_p} = C_L \frac{A + 4}{A + 4 \cos \Lambda} \left[1 + 6 \left(1 + \frac{\cos \Lambda}{A} \right) \frac{\tan^2 \Lambda}{12} \right] \left(\frac{C_{n_p}}{C_L} \right)_{\Lambda = 0^\circ}$$

Yawing Flight

An unsymmetrical spanwise distribution of load exists on a swept wing in yawing flight because of the velocity gradient along the span and because of the variation in direction of the air stream along the span. The primary force coefficients obtained for the condition of sideslipping flight can be modified for application to the case of yawing flight by letting β' be the angle between the plane of symmetry and the local air-stream direction at the quarter chord of any section and by accounting for the effect of the local velocity V' on the section coefficients. The section primary force coefficients, therefore, become

$$c_{l_L} = C_L \left(1 - \frac{A + 2 \cos \Lambda}{A + 4 \cos \Lambda} \beta' \tan \Lambda \right) \left(\frac{V'_L}{V} \right)^2 \tag{32}$$

$$c_{l_R} = C_L \left(1 + \frac{A + 2 \cos \Lambda}{A + 4 \cos \Lambda} \beta' \tan \Lambda \right) \left(\frac{V'_R}{V} \right)^2 \tag{33}$$

$$c_{2_L} = \frac{c_{l_L}^2}{\pi A \cos \Lambda} \left(1 + \frac{A + 8 \cos \Lambda}{A + 4 \cos \Lambda} \beta' \tan \Lambda \right) \left(\frac{V'_L}{V} \right)^2 \tag{34}$$

and

$$c_{2_R} = \frac{c_{l_R}^2}{\pi A \cos \Lambda} \left(1 - \frac{A + 8 \cos \Lambda}{A + 4 \cos \Lambda} \beta' \tan \Lambda \right) \left(\frac{V'_R}{V} \right)^2 \tag{35}$$

where β' and the velocity ratios are related to the yawing parameter $\frac{rb}{2V}$ by the equations

$$\beta' = -\frac{rb}{2V} \left[\frac{\bar{x}}{b/2} + \left(\frac{y}{b/2} - \frac{1}{2} \right) \tan \Lambda \right]$$

$$\frac{V'_L}{V} = 1 + \frac{y}{b/2} \frac{rb}{2V}$$

and

$$\frac{V'_R}{V} = 1 - \frac{y}{b/2} \frac{rb}{2V}$$

Rolling moment.- The coefficient of the rolling moment due to yawing is given by

$$C_l = \frac{1}{b^2}\int_0^{b/2} \left(c_{l_L} - c_{l_R}\right) y \, dy \tag{36}$$

By means of equations (32) and (33), it can be shown that

$$c_{l_L} - c_{l_R} = C_L \frac{rb}{2V}\left\{4\frac{y}{b/2} + 2\frac{A + 2\cos\Lambda}{A + 4\cos\Lambda}\tan\Lambda\left[\frac{\bar{x}}{b/2} + \left(\frac{y}{b/2} - \frac{1}{2}\right)\tan\Lambda\right]\right\}$$

and by substituting this value of $c_{l_L} - c_{l_R}$ in equation (36), the derivative of rolling moment due to yawing obtained is

$$C_{l_r} = C_L\left[\frac{1}{3} + \frac{A + 2\cos\Lambda}{A + 4\cos\Lambda}\left(\frac{\tan^2\Lambda}{24} + \frac{\bar{x}}{\bar{c}}\frac{\tan\Lambda}{2A}\right)\right]$$

or

$$C_{l_r} = C_L\left[1 + \frac{A + 2\cos\Lambda}{A + 4\cos\Lambda}\left(\frac{\tan^2\Lambda}{8} + \frac{3}{2}\frac{\bar{x}}{\bar{c}}\frac{\tan\Lambda}{A}\right)\right]\left(\frac{C_{l_r}}{C_L}\right)_{\Lambda=0^\circ} \tag{37}$$

Lateral force.- The coefficient of lateral force due to yawing is given by

$$C_Y = \frac{1}{b}\int_0^{b/2}\left[\left(c_{2_L} - c_{2_R}\right)\sin\Lambda - \left(c_{l_L}\theta_L - c_{l_R}\theta_R\right)\right]dy \tag{38}$$

where

$$\theta_L = \alpha\frac{\sin\Lambda}{\cos(\Lambda + \beta')}$$

and

$$\theta_R = \alpha\frac{\sin\Lambda}{\cos(\Lambda - \beta')}$$

From equations (34) and (35),

$$c_{2_L} - c_{2_R} = \frac{2C_L^2}{\pi A\cos\Lambda}\frac{rb}{2V}\left\{2\frac{y}{b/2} - \tan\Lambda\frac{A + 8\cos\Lambda}{A + 4\cos\Lambda}\left[\frac{\bar{x}}{b/2} + \left(\frac{y}{b/2} - \frac{1}{2}\right)\tan\Lambda\right]\right\}$$

and from equations (32) and (33) and by use of the relation between C_L and α as given by equation (6) with a_o equal to 2π,

$$c_{l_L}\theta_L - c_{l_R}\theta_R = \frac{C_L{}^2 \tan \Lambda}{\pi A \cos \Lambda}(A + 2 \cos \Lambda)\frac{rb}{2V}\left\{2\frac{y}{b/2} - \frac{2 \sin \Lambda}{A + 4 \cos \Lambda}\left[\frac{x}{b/2} + \left(\frac{y}{b/2} - \frac{1}{2}\right)\tan \Lambda\right]\right\}$$

After substituting these relations in equation (38) and integrating, the derivative of lateral force due to yawing for wings having taper ratios near 1.0 is found to be

$$C_{Y_r} = -C_L{}^2\frac{\tan \Lambda}{\pi A}\left[\frac{A}{2 \cos \Lambda} + 12\frac{x}{\bar{c}}\frac{\sin \Lambda}{A(A + 4 \cos \Lambda)}\right] \tag{39}$$

Yawing moment.- Yawing moment due to yawing results from the lift and induced forces and from an unsymmetrical spanwise distribution of profile drag. The increment of yawing moment due to yawing resulting from the lift and induced forces is given by the following equation:

$$\left(\Delta C_n\right)_1 = -\frac{1}{b^2}\int_0^{b/2}\left[\left(c_{2_L} - c_{2_R}\right)\left(y \cos \Lambda + x \sin \Lambda\right) - \left(c_{l_L}\theta_L - c_{l_R}\theta_R\right)x - \left(c_{l_L}\theta_L + c_{l_R}\theta_R\right)\beta' y\right]dy \tag{40}$$

From equations (32) and (33) and the relation between C_L and α as given by equation (6) with a_o equal to 2π, it can be shown that, to a first approximation,

$$c_{l_L}\theta_L + c_{l_R}\theta_R = \frac{1}{4} C_L{}^2 \frac{A + 2 \cos \Lambda}{\pi A \cos \Lambda} \tan \Lambda$$

The strip-theory value of the derivative is found, after appropriate substitutions for the quantities $c_{2_L} - c_{2_R}$, $c_{l_L}\theta_L - c_{l_R}\theta_R$, and $c_{l_L}\theta_L + c_{l_R}\theta_R$ in equation (40), to be

$$\left(\Delta C_{n_r}\right)_1 = -\frac{C_L^2}{2\pi A}\left\{\frac{2}{3} - \left(\frac{4\cos\Lambda}{A + 4\cos\Lambda} + \frac{A}{2\cos\Lambda}\right)\left(\frac{\bar{x}}{\bar{c}}\frac{\tan\Lambda}{A} + \frac{\tan^2\Lambda}{12}\right) - \frac{6\cos\Lambda}{A + 4\cos\Lambda}\left[4\left(\frac{\bar{x}}{\bar{c}}\right)^2\frac{\tan^2\Lambda}{A^2} + \frac{\tan^4\Lambda}{12}\right]\right\}$$

which can be written as

$$\left(\Delta C_{n_r}\right)_1 = C_L^2\left\{1 - \frac{3}{2}\left(\frac{4\cos\Lambda}{A + 4\cos\Lambda} + \frac{A}{2\cos\Lambda}\right)\left(\frac{\bar{x}}{\bar{c}}\frac{\tan\Lambda}{A} + \frac{\tan^2\Lambda}{12}\right) - \frac{9\cos\Lambda}{A + 4\cos\Lambda}\left[4\left(\frac{\bar{x}}{\bar{c}}\right)^2\frac{\tan^2\Lambda}{A^2} + \frac{\tan^4\Lambda}{12}\right]\right\}\left[\frac{\left(\Delta C_{n_r}\right)_1}{C_L^2}\right]_{\Lambda=0^\circ}$$

The wing profile drag, which has been neglected in the previous derivations given herein, may contribute an appreciable increment of yawing moment due to yawing. An accurate indication of the effects of profile drag on C_{n_r} can be obtained only when the spanwise distribution of profile drag is known. As an approximation, however, the profile drag may be assumed constant over the wing surface, in which case the quantity $\frac{\left(\Delta C_{n_r}\right)_2}{C_{D_o}}$ is a function only of the wing geometry. Such an assumption was made in reference 5. Calculations based on the methods given in reference 5 have been made for wings of the type considered in the present analysis. The results are given in figure 14.

The total value of the yawing moment due to yawing is the sum of the two increments that have been discussed. The complete equation for the derivative therefore is

$$C_{n_r} = C_L^2\left\{1 - \frac{3}{2}\left(\frac{4\cos\Lambda}{A + 4\cos\Lambda} + \frac{A}{2\cos\Lambda}\right)\left(\frac{\bar{x}}{\bar{c}}\frac{\tan\Lambda}{A} + \frac{\tan^2\Lambda}{12}\right) - \frac{9\cos\Lambda}{A + 4\cos\Lambda}\left[4\left(\frac{\bar{x}}{\bar{c}}\right)^2\frac{\tan^2\Lambda}{A^2} + \frac{\tan^4\Lambda}{12}\right]\right\}\left[\frac{\left(\Delta C_{n_r}\right)_1}{C_L^2}\right]_{\Lambda=0^\circ} + C_{D_o}\left[\frac{\left(\Delta C_{n_r}\right)_2}{C_{D_o}}\right] \quad (41)$$

As an approximation, the profile-drag coefficient may be assumed to be given by

$$C_{D_o} = C_D - \frac{C_L^2}{\pi A}$$

Pitching Flight

Lift.- If the center of gravity of an airplane does not coincide with the aerodynamic center, an increment of lift due to pitching arises from the change in the angle of attack at the aerodynamic center. The change in angle of attack is

$$(\Delta\alpha)_1 = 2\,\frac{qc}{2V}\,\frac{\bar{x}}{\bar{c}}$$

and the increment of lift is

$$(\Delta C_L)_1 = (\Delta\alpha)_1 C_{L_\alpha}$$

or

$$(\Delta C_L)_1 = 2\,\frac{qc}{2V}\,\frac{\bar{x}}{\bar{c}}\,C_{L_\alpha} \tag{42}$$

A second increment of lift due to pitching results from the curvature of the streamlines along the wing chord. The effect of streamline curvature on the lift of a wing is very similar to the effects of camber of a wing in straight flight. For an airfoil with circular camber, zero lift is obtained when the relative wind is approximately parallel to the tangent of the mean camber line at the three-quarter-chord station. The effective change in angle of attack, therefore, is the change in direction of flow between the one-half-chord station and the three-quarter-chord station. The change in angle of attack is

$$(\Delta\alpha)_2 = \frac{1}{2}\,\frac{qc}{2V}$$

For an infinite wing, the lift increment caused by curvature is simply

$$(\Delta C_L)_2 = \frac{1}{2}\,\frac{qc}{2V}\,a_o \cos\Lambda \tag{43}$$

and acts at the midchord station. For a finite wing, however, the increment of lift $(\Delta C_L)_2$ caused by curvature induces a lift force which acts at the quarter-chord station and is opposite in direction from $(\Delta C_L)_2$. The magnitude of the third lift increment due to pitching is given by

$$(\Delta C_L)_3 = -\frac{1}{2}\,\frac{qc}{2V}\left(a_o \cos\Lambda - C_{L_\alpha}\right) \tag{44}$$

The resultant lift-force increment due to pitching is found by adding equations (42), (43), and (44). The resulting equation is

$$C_{L_q} = \left(\frac{1}{2} + \frac{2\bar{x}}{\bar{c}}\right)C_{L_\alpha} \tag{45}$$

Pitching moment.- An increment of pitching moment due to pitching results from the lift due to pitching which was considered in the previous section. Thus

$$(\Delta C_m)_1 = -(\Delta C_L)_1 \frac{\bar{x}}{\bar{c}} - (\Delta C_L)_2 \left(\frac{\bar{x}}{\bar{c}} + \frac{1}{4}\right) - (\Delta C_L)_3 \frac{\bar{x}}{\bar{c}}$$

which, by substitution of equations (42) to (44), becomes

$$(\Delta C_m)_1 = \frac{qc}{2V}\left\{-C_{L_\alpha}\left[2\left(\frac{\bar{x}}{\bar{c}}\right)^2 + \frac{1}{2}\frac{\bar{x}}{\bar{c}}\right] - \frac{1}{8}a_o \cos \Lambda\right\}$$

or

$$\left(\Delta C_{m_q}\right)_1 = -C_{L_\alpha}\left[2\left(\frac{\bar{x}}{\bar{c}}\right)^2 + \frac{1}{2}\frac{\bar{x}}{\bar{c}}\right] - \frac{1}{8}a_o \cos \Lambda \qquad (46)$$

A second increment of pitching moment due to pitching is a moment about the aerodynamic center caused by a variation in angle of attack along the lifting line of the wing. This increment is not associated with a change in lift. For untapered wings the local difference between the angle of attack at any spanwise station on the lifting line and the angle of attack at the aerodynamic center is

$$(\Delta\alpha)_{local} = -\frac{2}{c}\frac{qc}{2V}\left(y - \frac{b}{4}\right)\tan \Lambda \qquad (47)$$

The incremental wing pitching moment can be found by an integration of the section pitching moments (about the wing aerodynamic center) along the wing span. For untapered wings

$$(\Delta C_m)_2 = K\frac{2}{S}a_o\int_0^{b/2}(\Delta\alpha)_{local}x'\,dy \qquad (48)$$

where K is a correction factor for the effects of finite aspect ratio on the local section lift coefficients. The expression for K cannot be determined exactly. A comparison of the angle-of-attack distribution for wings in pitching flight with the angle-of-attack distributions for wings in straight and rolling flight, however, indicates that the induced angle resulting from the pitching load should be approximately three times as large as the induced angle for a wing in straight flight. Thus,

$$K \approx \frac{A \cos \Lambda}{A + 6 \cos \Lambda}$$

Substitution of this approximation and of equation (47) in equation (48) gives

$$(\Delta C_m)_2 = -\frac{A \cos \Lambda}{A + 6 \cos \Lambda} \frac{2}{S} a_o \frac{qc}{2V} \frac{2}{\bar{c}} \int_0^{b/2} \left(y - \frac{b}{4}\right)^2 \tan^2 \Lambda \, dy$$

which, on performing the integration and solving for the derivative of pitching moment due to pitching, becomes

$$\left(\Delta C_{m_q}\right)_2 = -\frac{1}{24} \frac{A^3 a_o \cos \Lambda}{A + 6 \cos \Lambda} \tan^2 \Lambda \tag{49}$$

The total value of the derivative of pitching moment due to pitching is obtained by adding equation (46) and equation (49). Thus,

$$C_{m_q} = -C_{L_\alpha} \left[2\left(\frac{\bar{x}}{\bar{c}}\right)^2 + \frac{1}{2} \frac{\bar{x}}{\bar{c}} \right] - \frac{1}{8} a_o \cos \Lambda - \frac{1}{24} \frac{A^3 a_o \cos \Lambda}{A + 6 \cos \Lambda} \tan^2 \Lambda$$

Substitution of the expression for C_{L_α} given by equation (6), and rearranging, leads to

$$C_{m_q} = -a_o \cos \Lambda \left\{ \frac{A\left[2\left(\frac{\bar{x}}{\bar{c}}\right)^2 + \frac{1}{2} \frac{\bar{x}}{\bar{c}}\right]}{A + 2 \cos \Lambda} + \frac{1}{24} \frac{A^3 \tan^2 \Lambda}{A + 6 \cos \Lambda} + \frac{1}{8} \right\} \tag{50}$$

Values of C_{m_q} have been derived by Glauert (reference 6) for rectangular unswept wings, and these values might be used as a basis for a general equation that includes the derivative for the unswept wing as has been done in several of the previous derivations. It is found, however, upon setting a_o equal to 2π, that equation (50) gives values for C_{m_q} for unswept wings that are very nearly the same as those given by the more exact method of reference 6. There seems to be no advantage, therefore, in altering the form of equation (50).

DISCUSSION

The derived expressions for the stability derivatives of swept wings are summarized in tabls I. All those expressions (equations for C_{L_α}, C_{l_β}, C_{l_p}, C_{n_p}, C_{l_r}, and C_{n_r}) that have been related to the derivatives for an unswept wing of the same aspect ratio and taper ratio as the swept wing are considered to be applicable to wings having taper ratios ranging

at least from 1.0 to 0.5. For those expressions in which the simple theory has been used to determine the absolute magnitudes of the derivatives (equations for C_{n_β}, C_{Y_β}, C_{Y_p}, C_{Y_r}, C_{l_q}, and C_{m_q}), the derivations have been made specifically for a taper ratio of 1.0. In most instances, however, moderate deviations from a taper ratio of 1.0 are not likely to have any large effect on the values of the derivatives, at least for low lift coefficients.

The expressions included in table I have been used to derive charts (figs. 4 to 15) that give values of the derivatives as functions of sweep angle, aspect ratio, and center-of-gravity location for wings with taper ratio of 1.0. Whenever a choice of the section lift-curve slope could be made, a value of 5.67 (per radian) was assumed as in reference 7. The charts are presented primarily for illustrating the effects of the most important variables. The equations normally should be used when making estimates for a specific wing, since, at least for the more important derivatives, the taper ratio and section lift-curve slope may then be considered in evaluating the derivatives.

The wing contribution to the derivatives C_{Y_β}, C_{n_β}, C_{Y_p}, and C_{Y_r}, which generally is neglected in the case of unswept wings, has been considered in the present analysis in order to indicate at least the order of magnitude of the effects of sweep. The analysis indicates that these derivatives are affected by sweep, but the effect probably is not particularly important unless very large sweep angles are used.

Experimental data for the derivatives have been obtained for the series of untapered swept wings shown in figure 16. The tests were made in the Langley stability tunnel by a procedure in which the air stream is made to roll or curve about a stationary model. Comparison of experimental results and results calculated by the methods developed herein are shown in figures 17 to 21.

The characteristics of the unswept wing were generally predicted quite accurately at all lift coefficients below the stall - probably because no important deviations from potential-flow characteristics are likely to occur with unswept wings of moderate and high aspect ratio until maximum lift is approached.

The approximate theory generally indicates accurately the trends resulting from the effects of sweep, at least over a range of lift coefficient (starting from zero) that decreases as the sweep angle increases. In some instances, however, particularly for the derivatives C_{n_p} and C_{l_r}, the theory appears to underestimate the magnitudes of the effects of sweep. This underestimation probably results largely from the fact that changes in the span-load distributions are not accounted for in the present analytical method.

At high lift coefficients, poor agreement between experimental and calculated derivatives frequently was obtained for the swept wings. The damping in roll, for example, increased considerably with lift coefficient

for all the swept wings tested. This increase cannot be considered to be a characteristic trend for swept wings, however, since tests of highly tapered swept wings have indicated marked reductions in the damping in roll as the lift coefficient increased. It should be noted that the signs of the rather important derivatives Cn_p and C_{l_r} were reversed in the high lift-coefficient range.

The large discrepancies between calculated and experimental results for highly swept wings at moderate and high lift coefficients undoubtedly are caused by partial separation of flow which results in changes in the distributions of lift and drag along the wing span. Increases in Reynolds number (tests were made at Reynolds numbers ranging from 1,000,000 to 2,000,000) probably would delay the alterations in the flow conditions. Even at high Reynolds numbers, however, trends similar to those shown by the experimental data probably would occur, although the breaks in the curves may be delayed to higher lift coefficients.

The observations made in comparing experimental and calculated derivatives indicate that the analytical assumptions normally made for unswept wings throughout the lift-coefficient range are likely to be inadequate for swept wings, particularly at moderate and high lift coefficients. Although important simplifications were introduced in developing the present analytical method, this simplified method appears to be justified because even the most rigorous method, if based on potential-flow concepts, can be expected to give reliable results only over a limited lift-coefficient range. At high lift coefficients, a more rigorous method probably would provide very little improvement over the present method. Considerably more information about the characteristics of flow about swept wings at high lift coefficients is required before a reliable method can be developed for evaluating the derivatives throughout the lift-coefficient range.

CONCLUDING REMARKS

Approximate relations for the low-speed stability derivatives of swept wings are derived from a simplified theory. Comparison of values of the derivatives obtained from the approximate relations with values obtained by experiment indicates that the calculated values are fairly reliable over a range of lift coefficient (starting from zero) that decreases as the sweep angle increases. Large discrepancies between calculated and experimental values are found for highly swept wings at the high lift coefficients for which the flow is believed to be partially separated from the wing surfaces. Even a more rigorous method, if based on potential-flow concepts, probably would not provide much improvement in the range of lift coefficient for which partial separation exists.

Langley Memorial Aeronautical Laboratory
National Advisory Committee for Aeronautics
Langley Field, Va., January 30, 1948

APPENDIX

STABILITY DERIVATIVES OF UNSWEPT WINGS

The determination of the stability derivatives of swept wings according to the methods proposed in the present paper involves, in several cases, application of approximate corrections for the effects of sweep to values of the derivatives for unswept wings that have the same aspect ratio and taper ratio as the swept wings. In the absence of experimental data for the unswept wings, theoretical values must be used. In many instances, aspect ratios below the range that has been investigated by rigorous theoretical methods must be considered. This appendix presents methods of extending or of extrapolating the available theoretical values of the stability derivatives of unswept wings to low aspect ratios. For the various yawing-moment and rolling-moment derivatives, effective lateral centers of pressure are calculated by equating approximate relations for the derivatives to values of the derivatives that have been calculated by more rigorous methods. The curves obtained for the lateral centers of pressure are then extrapolated to low aspect ratios, and the derivatives are then calculated by means of the approximate relations for the complete range of aspect ratio. This procedure is considered to give more reliable results than could be obtained by extrapolating values of the derivatives themselves, since the lateral centers of pressure normally vary only slightly with aspect ratio, whereas the derivatives may vary considerably.

Lift-Curve Slope

An equation (given in reference 2) for the lift-curve slope is as follows:

$$C_{L_\alpha} = \frac{Aa_o}{AE_e + \frac{a_o}{\pi}} \tag{A1}$$

where E_e is a correction factor that accounts for differences between lifting-line and lifting-surface theories. For the theoretical value of a_o (equal to 2π), equation (A1) becomes

$$C_{L_\alpha} = \frac{2\pi A}{AE_e + 2} \tag{A2}$$

The edge-velocity correction factor E_e is given in figure 16 of reference 8 for aspect ratios from 2 to 16; therefore, the product AE_e may be calculated for the same range.

The lift-curve slopes for wings having very low aspect ratios (approaching zero) is, according to reference 4,

$$C_{L_\alpha} = \frac{\pi A}{2} \tag{A3}$$

By equating relations (A2) and (A3), the product AE_e is found to approach 2.0 as the aspect ratio approaches 0. A curve of the product AE_e, therefore, can be constructed for aspect ratios from 0 to 16. (See fig. 22.) These values for AE_e can be used in equation (A1) to calculate values of C_{L_α} throughout the aspect-ratio range.

Rolling Moment Due to Sideslip

A theoretical solution for the rolling moment due to sideslip has been obtained by Weissinger (reference 9). In general, Weissinger's results have been found to be in good agreement with experiment. Values of the quantity $\left(\frac{C_{l_\beta}}{C_L}\right)_{\Lambda=0^\circ}$ from reference 9 are presented in figure 23.

The lateral center of pressure $\bar{y}_{L'_\beta}$ associated with the antisymmetrical load on a swept wing in sideslip can be assumed, as a first approximation, to be equal to the lateral center of pressure of the load associated with dihedral for an unswept wing. The panels of an unswept wing undergo an angle-of attack change, in sideslip, given by

$$\Delta\alpha = \beta \tan \Gamma$$

From this relation, the rolling moment due to sideslip, per radian of dihedral, can be shown to be approximately

$$\frac{C_{l_\beta}}{\Gamma} = -\frac{1}{2}\frac{Aa_o}{A+4}\frac{\bar{y}_{L'_\beta}}{b/2}$$

Values of $\frac{\bar{y}_{L'_\beta}}{b/2}$ for wings having aspect ratios between 6 and 16 can be obtained by equating the expression just given to the values of $\frac{C_{l_\beta}}{\Gamma}$ given in figure 16 of reference 7. The results, extrapolated to an aspect ratio of 1.0, are presented in figure 23.

Yawing Moment Due to Sideslip

An unsymmetrical induced-drag distribution, associated with the unsymmetrical lift distribution, exists on an unswept wing in sideslip.

A yawing moment due to sideslip therefore results, which, according to Hoerner (reference 10), is given approximately by the relation

$$\left(\frac{\Delta C_{n_\beta}}{C_L^2}\right)_{\Lambda=0^\circ} = \frac{1}{4\pi A} \tag{A4}$$

Rolling Moment Due to Rolling

If the wing-panel loads of an unswept wing in roll are assumed to be concentrated at the lateral centers of pressure, the rolling moment due to rolling can be expressed as

$$C_l = \left(C_{l_L} - C_{l_R}\right)\frac{\bar{y}_L' p}{b}$$

where, by a development similar to that given in the section of the text on the rolling moment due to rolling of swept wings,

$$C_{l_L} = \frac{C_L}{2} - \frac{1}{2}\frac{Aa_o}{A + \frac{2a_o}{\pi}}\frac{\bar{y}_L' p}{b/2}\frac{pb}{2V}$$

and

$$C_{l_R} = \frac{C_L}{2} + \frac{1}{2}\frac{Aa_o}{A + \frac{2a_o}{\pi}}\frac{\bar{y}_L' p}{b/2}\frac{pb}{2V}$$

The derivative of rolling moment due to rolling, therefore, is

$$C_{l_p} = -\frac{1}{2}\frac{Aa_o}{A + \frac{2a_o}{\pi}}\left(\frac{\bar{y}_L' p}{b/2}\right)^2$$

which, with the lifting-surface-theory correction factor E_e' of reference 8, becomes

$$C_{l_p} = -\frac{1}{2}\frac{Aa_o}{AE_e' + \frac{2a_o}{\pi}}\left(\frac{\bar{y}_L' p}{b/2}\right)^2 \tag{A5}$$

For elliptic wings and a section lift-curve slope of 2π, reference 8 gives

$$C_{l_p} = -\frac{1}{4}\frac{\pi A}{AE_e' + 4} \tag{A6}$$

which is identical with equation (A5) when $\frac{\bar{y}_{L'_p}}{b/2}$ is equal to 0.5.

The rolling moment due to rolling of low-aspect-ratio triangular wings at small angles of attack is, according to reference 5,

$$C_{l_p} = -\frac{1}{32}\pi A \tag{A7}$$

Equation (A7) is expected to apply, at small angles of attack, to low-aspect-ratio wings of almost any plan form.

Equation (A6) is identical with equation (A7) provided that the product AE_e' is equal to 4.0. This value and values of E_e' given in reference 8 for aspect ratios greater than 2.5 have been used to construct the curve of the product AE_e' given in figure 22. Values of the lateral center of pressure $\frac{\bar{y}_{L'_p}}{b/2}$ were calculated for wings of aspect ratios greater than 6.0 by setting equation (A5) equal to the lifting-surface values of C_{l_p} given in reference 8. These results, given in figure 24, were extended to the value 0.5 which was previously found to satisfy equation (A6) for aspect ratios approaching zero. Since both the lateral center of pressure $\frac{\bar{y}_{L'_p}}{b/2}$ and the product AE_e' have now been evaluated for aspect ratios from 0 to 16, equation (A5) may be used to calculate C_{l_p} throughout this aspect-ratio range. The results of calculations based on a value of a_o equal to 5.67 are presented in figure 24.

Yawing Moment Due to Rolling

An equation for the yawing moment due to rolling of unswept wings, derived from wing-panel primary force coefficients instead of section primary force coefficients, is found to be

$$\frac{C_{n_p}}{C_L} = -\frac{1}{2}\frac{A}{A + 4}\left(\frac{\bar{y}_{N_p}}{b/2}\right)^2 \tag{A8}$$

This equation and values of C_{n_p} given in figure 9 of reference 7 were used to calculate values of $\frac{\bar{y}_{N_p}}{b/2}$ for wings having aspect ratios between 6 and 16. The results, plotted in figure 25, were extrapolated to an aspect ratio of 1.0. The extrapolated curves and equation (A8) were used to calculate the values of $\left(\frac{C_{n_p}}{C_L}\right)_{\Lambda=0^\circ}$ presented in figure 25.

Rolling Moment Due to Yawing

The rolling moment due to yawing for unswept wings is found, by a derivation based on wing-panel primary force coefficients, to be

$$\frac{C_{l_r}}{C_L} = \left(\frac{\bar{y}_{L'_r}}{b/2}\right)^2 \tag{A9}$$

Values of $\frac{\bar{y}_{L'_r}}{b/2}$ were calculated for aspect ratios ranging from 6 to 16 by means of equation (A9) and the values of C_{l_r} given in figure 11 of reference 7. The results, extrapolated to an aspect ratio of 1.0, are presented in figure 26. The extrapolated curves and equation (A9) were used to calculate the values of $\left(\frac{C_{l_r}}{C_L}\right)_{\Lambda=0^\circ}$ given in figure 26.

Yawing Moment Due to Yawing

The increment of yawing moment due to yawing of unswept wings, resulting from lift and induced drag, is found by a derivation based on wing-panel primary force coefficients to be given by the expression

$$\left(\Delta C_{n_r}\right)_1 = -\frac{C_L^2}{\pi A}\left(\frac{\bar{y}_{N_r}}{b/2}\right)^2 \tag{A10}$$

This equation and values of C_{n_r} from figure 12 of reference 7 (as corrected by errata sheet) were used to calculate values of $\frac{\bar{y}_{N_r}}{b/2}$ for aspect ratios from 6 to 16. Figure 27 presents values of $\frac{\bar{y}_{N_r}}{b/2}$ extrapolated to an aspect ratio of 1.0 and values of $\left[\frac{\left(\Delta C_{n_r}\right)_1}{C_L^2}\right]_{\Lambda=0^\circ}$ calculated from equation (A10) and the extrapolated curves.

REFERENCES

1. Betz, A: Applied Airfoil Theory. Unsymmetrical and Non-Steady Types of Motion, Vol. IV of Aerodynamic Theory, div. J, ch. IV, sec. 4, W. F. Durand, ed., Julius Springer (Berlin), 1935, pp. 102-107.

2. Swanson, Robert S., and Crandall, Stewart M.: Lifting-Surface-Theory Aspect-Ratio Corrections to the Lift and Hinge-Moment Parameters for Full-Span Elevators on Horizontal Tail Surfaces. NACA TN No. 1175, 1947.

3. Mutterperl, William: The Calculation of Span Load Distributions on Swept-Back Wings. NACA TN No. 834, 1941.

4. Jones, Robert T.: Properties of Low-Aspect-Ratio Pointed Wings at Speeds below and above the Speed of Sound. NACA TN No. 1032, 1946.

5. Ribner, Herbert S.: The Stability Derivatives of Low-Aspect-Ratio Triangular Wings at Subsonic and Supersonic Speeds. NACA TN No. 1423, 1947.

6. Glauert, H.: The Lift and Pitching Moment of an Aerofoil Due to a Uniform Angular Velocity of Pitch. R. & M. No. 1216, British A.R.C., 1929.

7. Pearson, Henry A., and Jones, Robert T.: Theoretical Stability and Control Characteristics of Wings with Various Amounts of Taper and Twist. NACA Rep. No. 635, 1938.

8. Swanson, Robert S., and Priddy, E. LaVerne: Lifting-Surface-Theory Values of the Damping in Roll and of the Parameter Used in Estimating Aileron Stick Forces. NACA ARR No. L5F23, 1945.

9. Weissinger, J: Der schiebende Tragflügel bei gesunder Strömumg. Bericht S 2 der Lilienthal-Gesellschaft für Luftfahrtforschung, 1938-39, pp. 13-51.

10. Hoerner, Sighard: Forces and Moments on a Yawed Airfoil. NACA TM No. 906, 1939.

TABLE I.- SUMMARY OF APPROXIMATE RELATIONS FOR STABILITY DERIVATIVES OF SWEPT WINGS

Derivative	Relation	Equation	Figure $\lambda \approx 1.0$	Remarks
C_{L_α}	$\frac{(A+2)\cos\Lambda}{A+2\cos\Lambda}\left(C_{l_\alpha}\right)_{\Lambda=0^\circ}$	(7)	4	$\left(C_{l_\alpha}\right)_{\Lambda=0^\circ}$ from equation (A1)
C_{l_β}	$C_L\left[\left(\frac{\Delta C_{l_\beta}}{C_L}\right)_{\Lambda=0^\circ}-\frac{\bar{y}_{L'_\beta}}{b/2}\frac{A+2\cos\Lambda}{A+4\cos\Lambda}\frac{\tan\Lambda}{2}\right]$	(17)	5	$\left(\frac{\Delta C_{l_\beta}}{C_L}\right)_{\Lambda=0^\circ}$ and $\frac{\bar{y}_{L'_\beta}}{b/2}$ from fig. 23
C_{Y_β}	$C_L{}^2\frac{6\tan\Lambda\sin\Lambda}{\pi A(A+4\cos\Lambda)}$	(19)	6	Derived for $\lambda \approx 1.0$
C_{n_β}	$C_L{}^2\left[\left(\frac{\Delta C_{n_\beta}}{C_L{}^2}\right)_{\Lambda=0^\circ}-\frac{\tan\Lambda}{\pi A(A+4\cos\Lambda)}\left(\cos\Lambda-\frac{A}{2}-\frac{A^2}{8\cos\Lambda}+6\frac{\bar{x}}{b}\frac{\sin\Lambda}{A}\right)\right]$	(21)	7	$\left(\frac{\Delta C_{n_\beta}}{C_L{}^2}\right)_{\Lambda=0^\circ}$ from equation (A4) Derived for $\lambda \approx 1.0$
C_{l_p}	$\frac{(A+4)\cos\Lambda}{A+4\cos\Lambda}\left(C_{l_p}\right)_{\Lambda=0^\circ}$	(27)	8	$\left(C_{l_p}\right)_{\Lambda=0^\circ}$ from equation (A5)
C_{Y_p}	$C_L\frac{A+\cos\Lambda}{A+4\cos\Lambda}\tan\Lambda$	(29)	9	Derived for $\lambda \approx 1.0$
C_{n_p}	$C_L\frac{A+4}{A+4\cos\Lambda}\left[1+6\left(1+\frac{\cos\Lambda}{A}\right)\left(\frac{\bar{x}}{b}\tan\Lambda+\frac{\tan^2\Lambda}{12}\right)\right]\left(\frac{C_{n_p}}{C_L}\right)_{\Lambda=0^\circ}$	(31)	10	$\left(\frac{C_{n_p}}{C_L}\right)_{\Lambda=0^\circ}$ from fig. 25
C_{l_r}	$C_L\left[1+\frac{A+2\cos\Lambda}{A+4\cos\Lambda}\left(\frac{\tan^2\Lambda}{8}+\frac{3}{2}\frac{\bar{x}}{c}\frac{\tan\Lambda}{A}\right)\right]\left(\frac{C_{l_r}}{C_L}\right)_{\Lambda=0^\circ}$	(37)	11	$\left(\frac{C_{l_r}}{C_L}\right)_{\Lambda=0^\circ}$ from fig. 26
C_{Y_r}	$-C_L{}^2\frac{\tan\Lambda}{\pi A}\left[\frac{A}{2\cos\Lambda}+12\frac{\bar{x}}{b}\frac{\sin\Lambda}{A(A+4\cos\Lambda)}\right]$	(39)	12	Derived for $\lambda \approx 1.0$
C_{n_r}	$C_L{}^2\left\{1-\frac{3}{2}\left(\frac{4\cos\Lambda}{A+4\cos\Lambda}+\frac{A}{2\cos\Lambda}\right)\left(\frac{\bar{x}}{b}\frac{\tan\Lambda}{A}+\frac{\tan^2\Lambda}{12}\right)-\frac{9\cos\Lambda}{A+4\cos\Lambda}\left[4\left(\frac{\bar{x}}{b}\right)^2\frac{\tan^2\Lambda}{A^2}+\frac{\tan^4\Lambda}{12}\right]\right\}\left[\frac{\left(\Delta C_{n_{p_1}}\right)_1}{C_L{}^2}\right]_{\Lambda=0^\circ}+C_{D_o}\left[\frac{\left(\Delta C_{n_{p_2}}\right)_2}{C_{D_o}}\right]$	(41)	13 and 14	$\left[\frac{\left(\Delta C_{n_{p_1}}\right)_1}{C_L{}^2}\right]_{\Lambda=0^\circ}$ from fig. 27
C_{L_q}	$\left(\frac{1}{2}+\frac{2\bar{x}}{c}\right)C_{L_\alpha}$	(45)	-	C_{L_α} from equation (7)
C_{m_q}	$-a_o\cos\Lambda\left\{\frac{A\left[2\left(\frac{\bar{x}}{c}\right)^2+\frac{1}{12}\frac{\bar{x}}{c}\right]}{A+2\cos\Lambda}+\frac{1}{24}\frac{A^3\tan^2\Lambda}{A+6\cos\Lambda}+\frac{1}{8}\right\}$	(50)	15	Derived for $\lambda \approx 1.0$

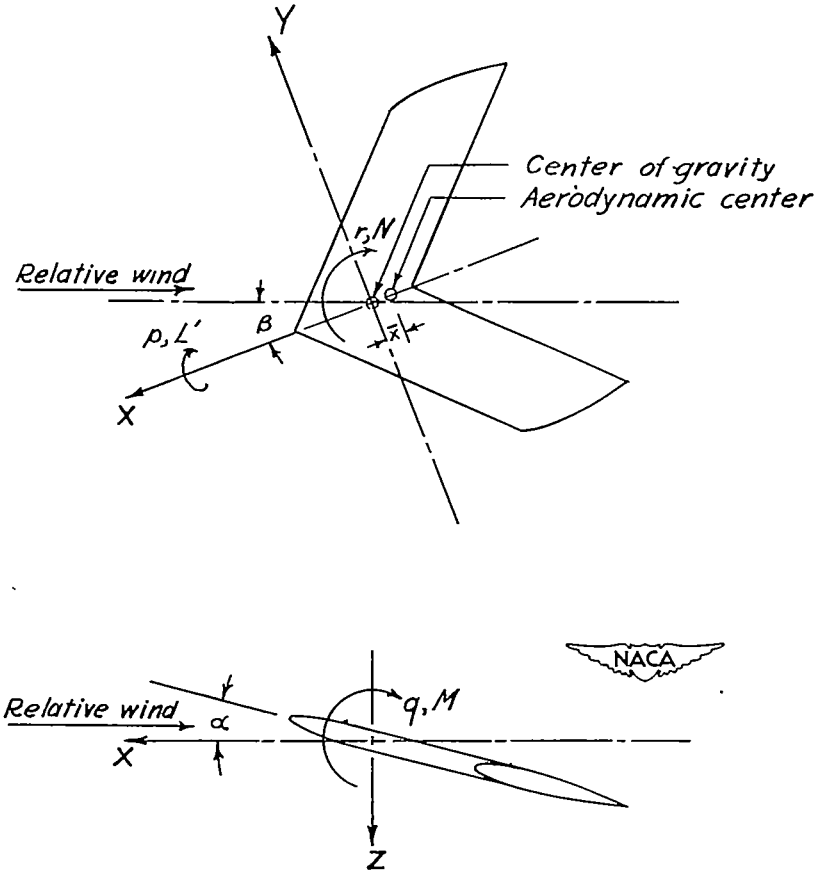

Figure 1.- Angular velocities and moments for stability-axes system.

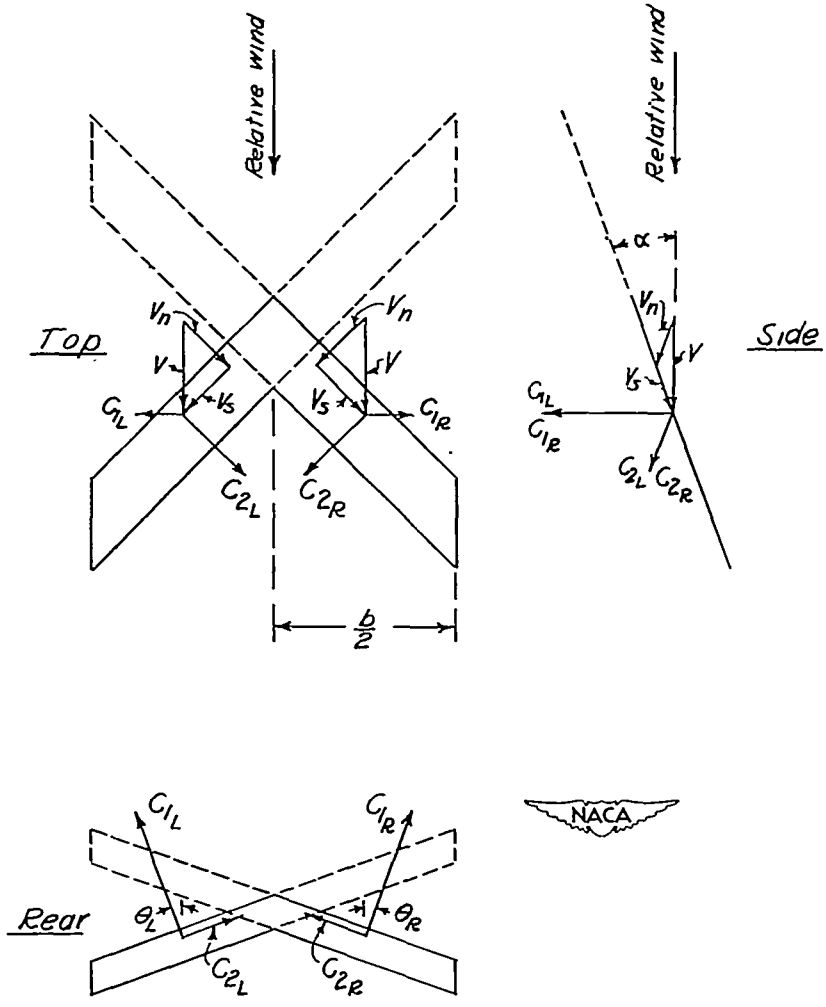

Figure 2.- Orientation of velocities and forces considered in swept-wing analysis.

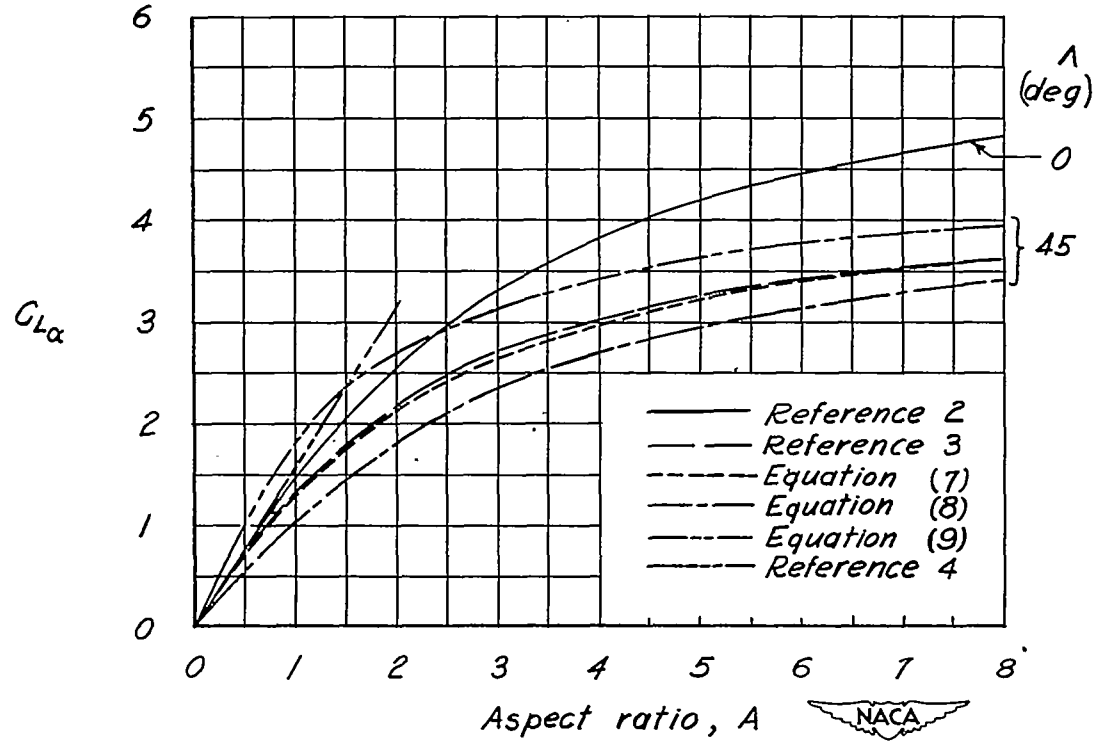

Figure 3.- Comparison of the variation of lift-curve slope with aspect ratio as calculated by several methods. $a_0 = 2\pi$.

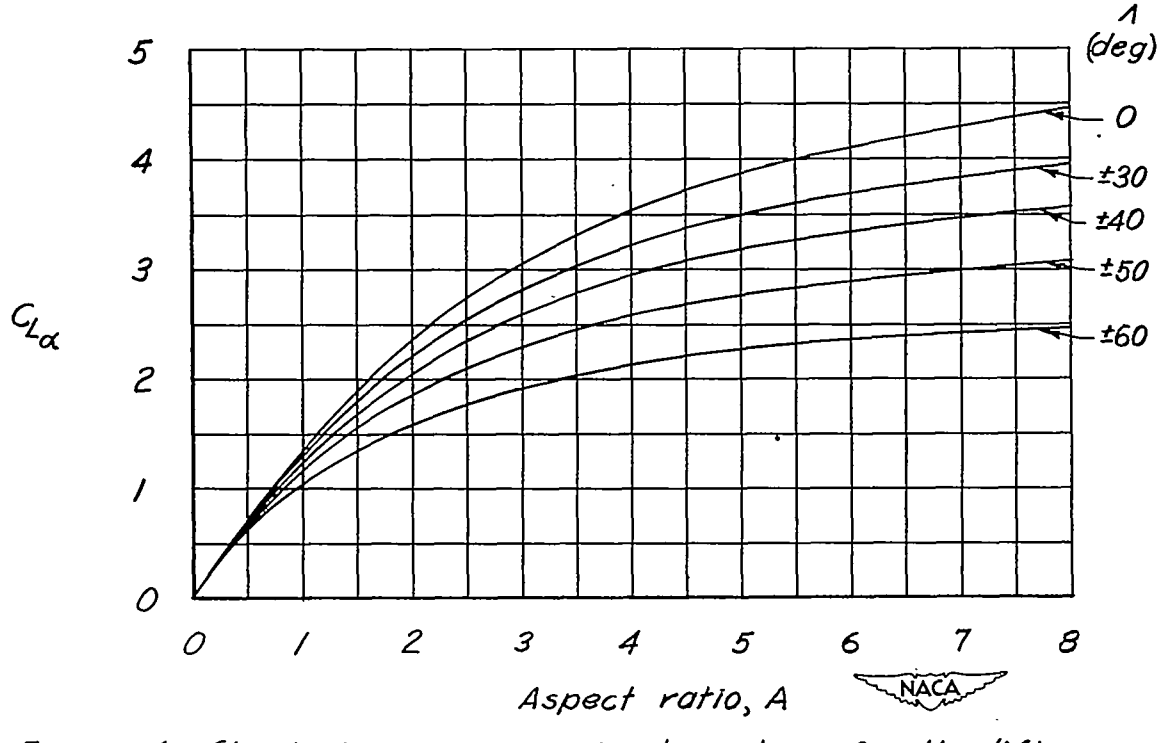

Figure 4.- Chart showing approximate values for the lift-curve slope given by equation (7). $a_0 = 5.67$.

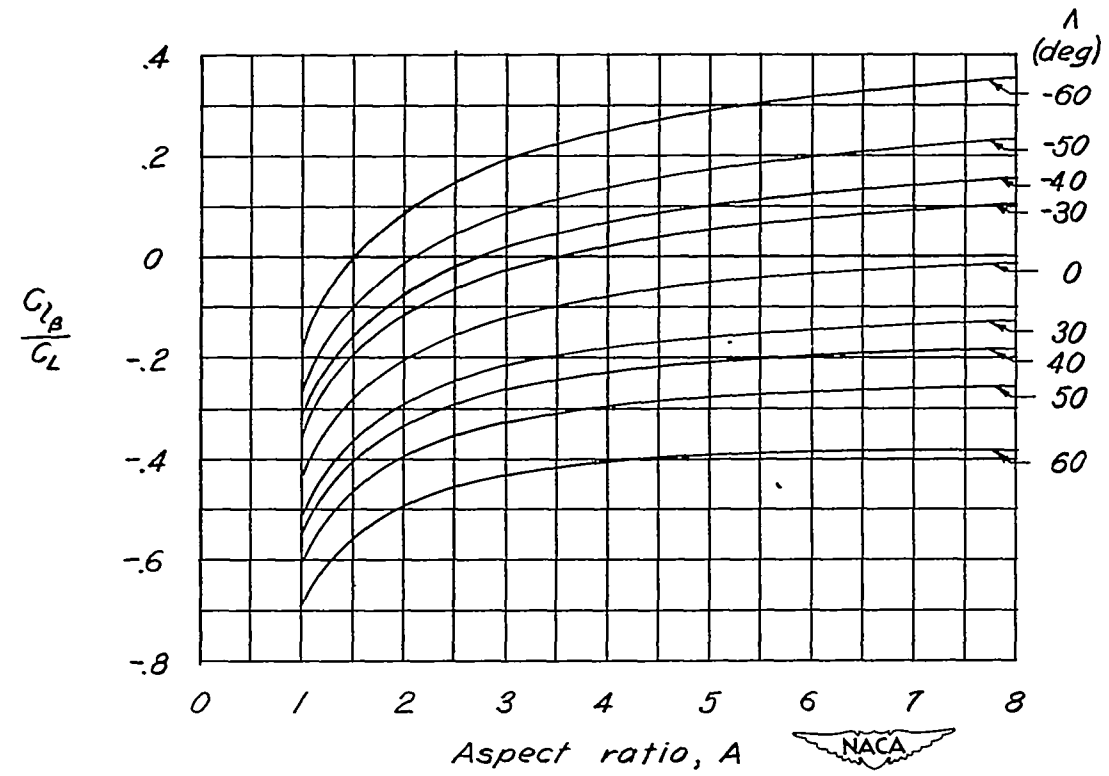

Figure 5.- Chart showing approximate values for the rolling moment due to sideslip given by equation (17). $\lambda = 1.0$.

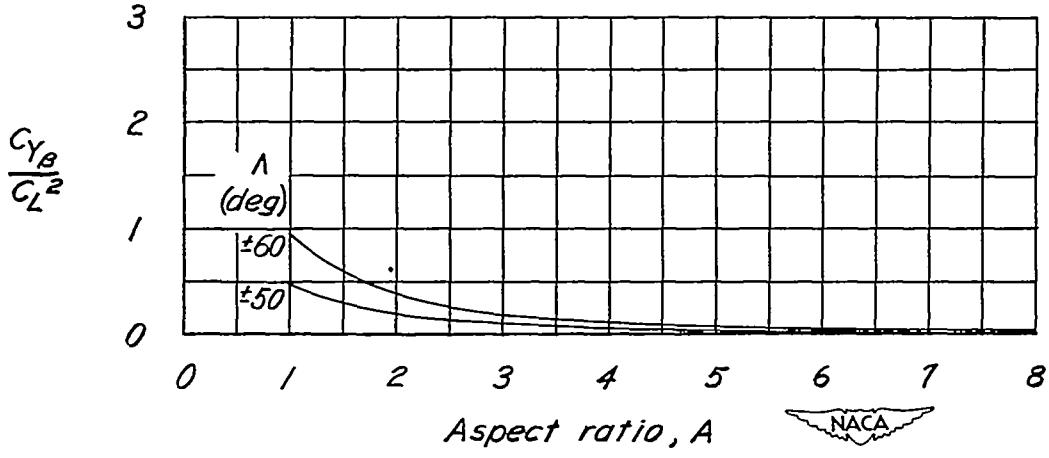

Figure 6.- Chart showing approximate values for the lateral force due to sideslip given by equation (19). $\lambda \approx 1.0$.

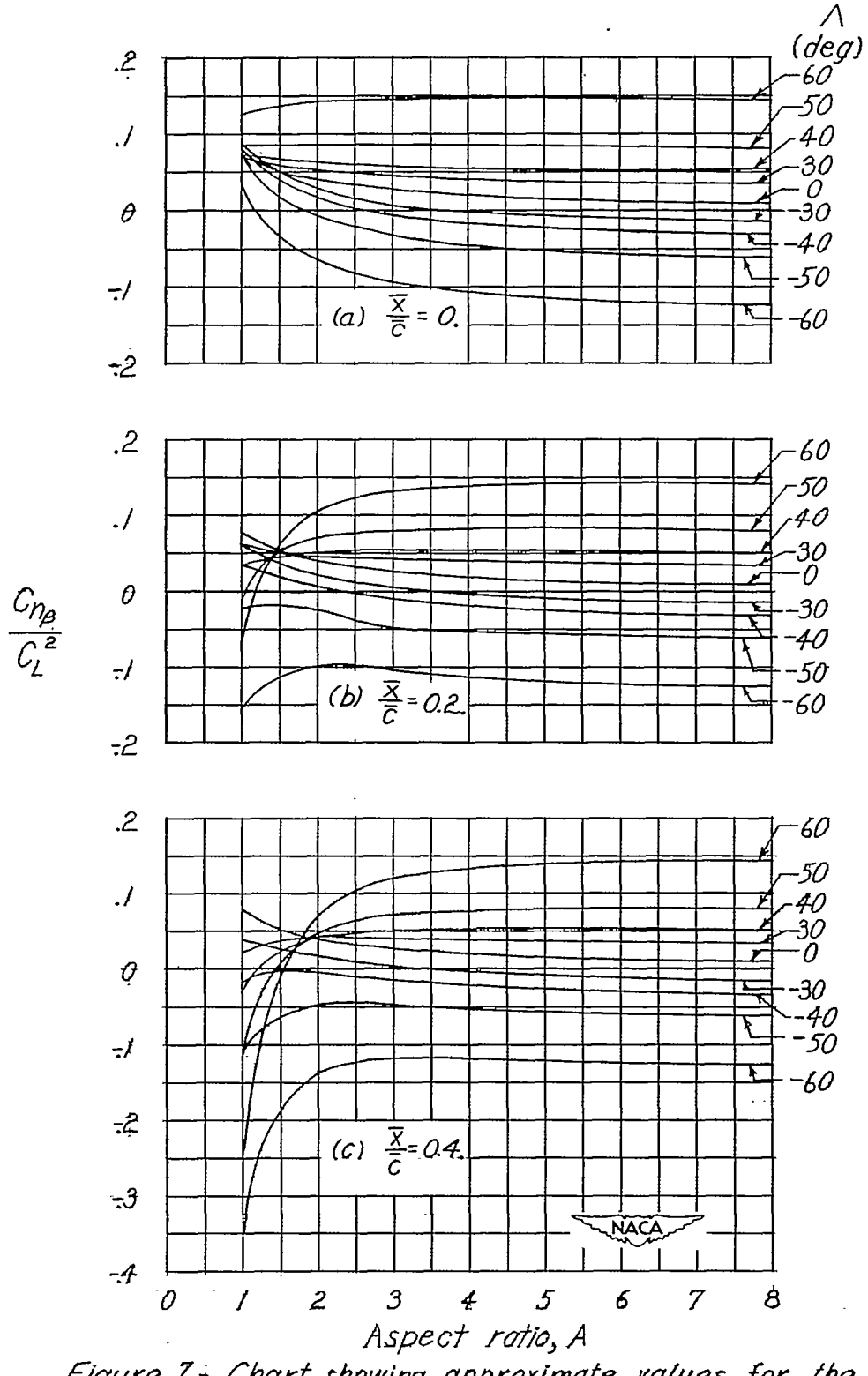

Figure 7.- Chart showing approximate values for the yawing moment due to sideslip given by equation (21). $\lambda \approx 1.0$.

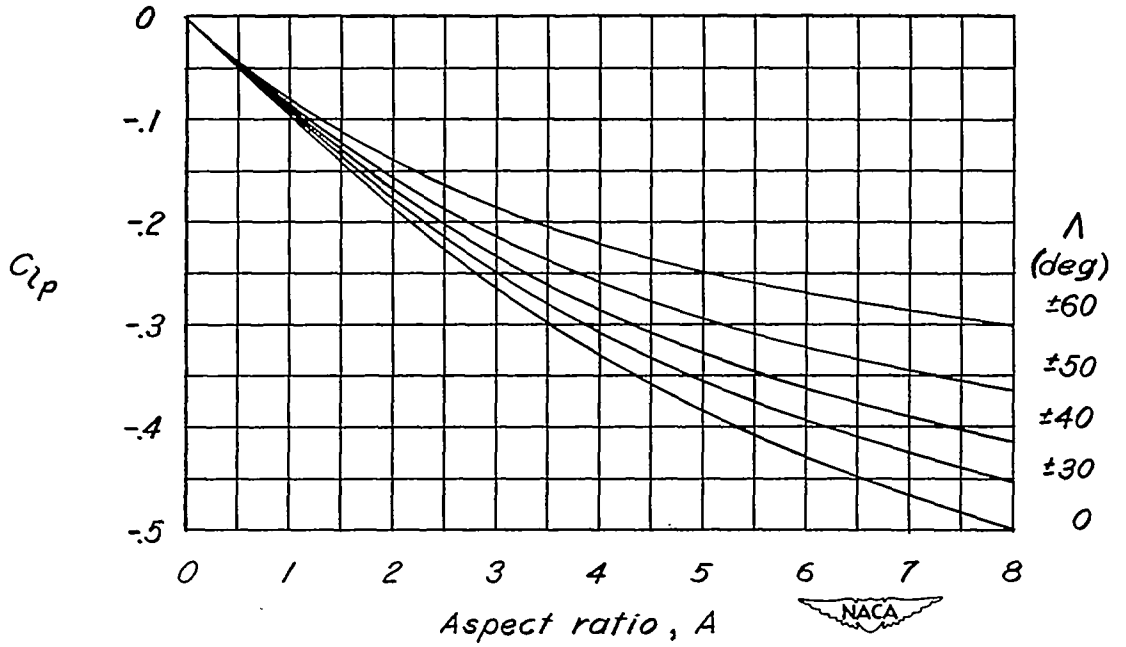

Figure 8.- Chart showing approximate values for the rolling moment due to rolling given by equation (27). $a_0 = 5.67$; $\lambda = 1.0$.

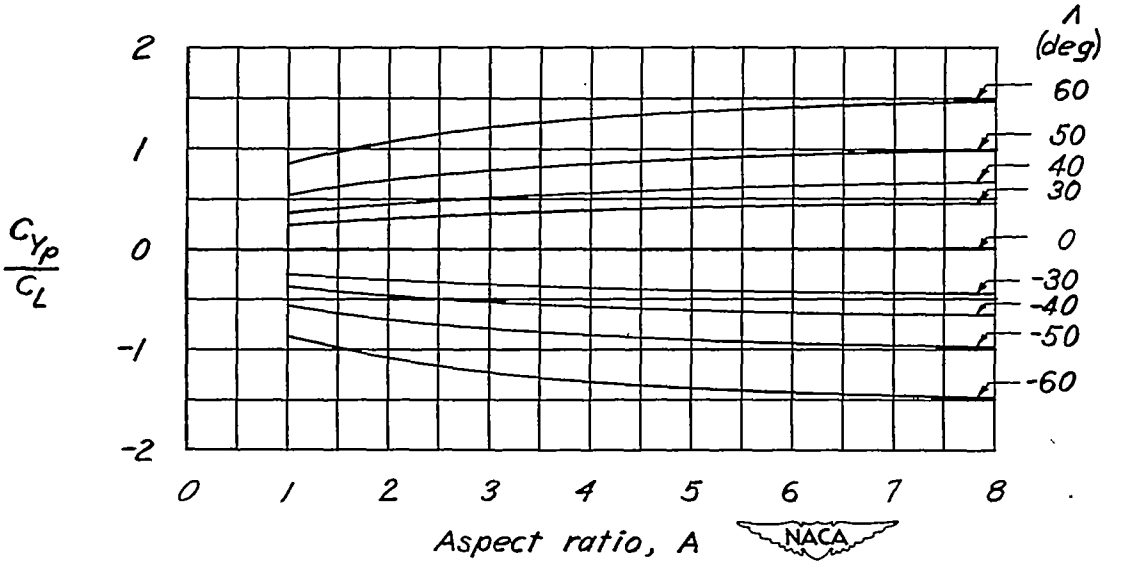

Figure 9.- Chart showing approximate values for the lateral force due to rolling given by equation (29). $\lambda \approx 1.0$.

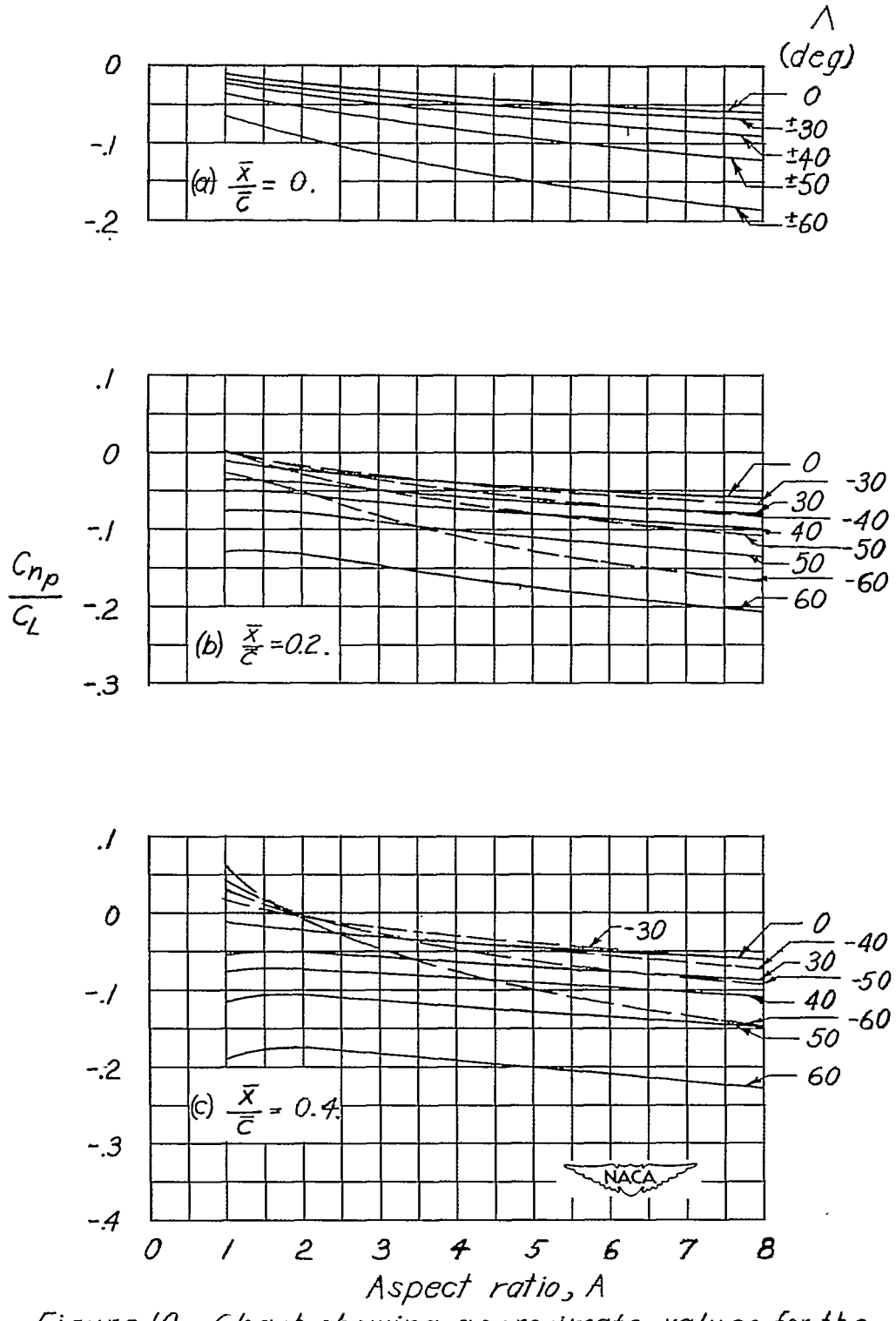

Figure 10.- Chart showing approximate values for the yawing moment due to rolling given by equation (31). $a_0 = 5.67$; $\lambda = 1.0$.

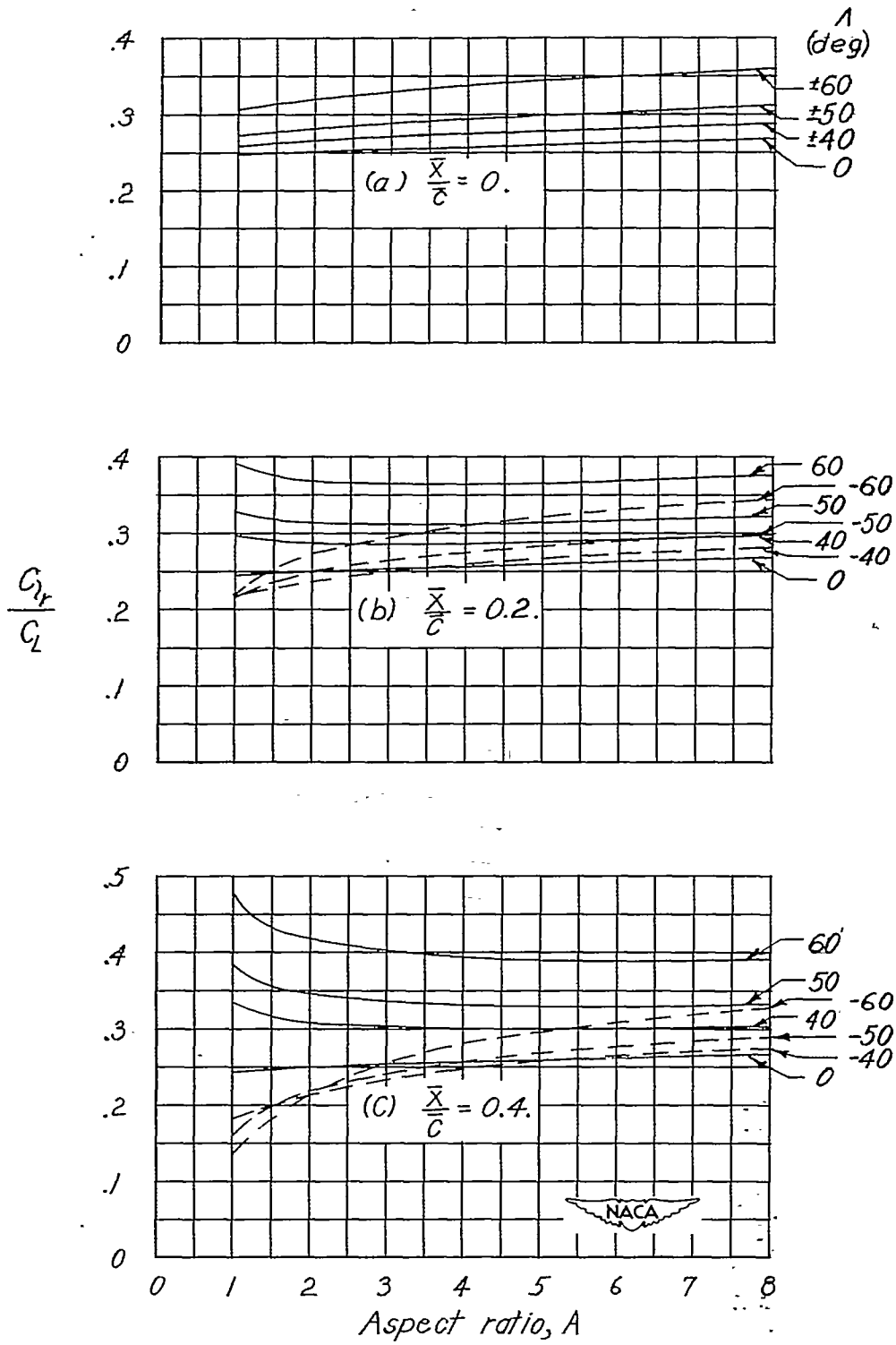

Figure 11.- Chart showing approximate values for the rolling moment due to yawing given by equation (37). $a_o = 5.67$; $\lambda = 1.0$.

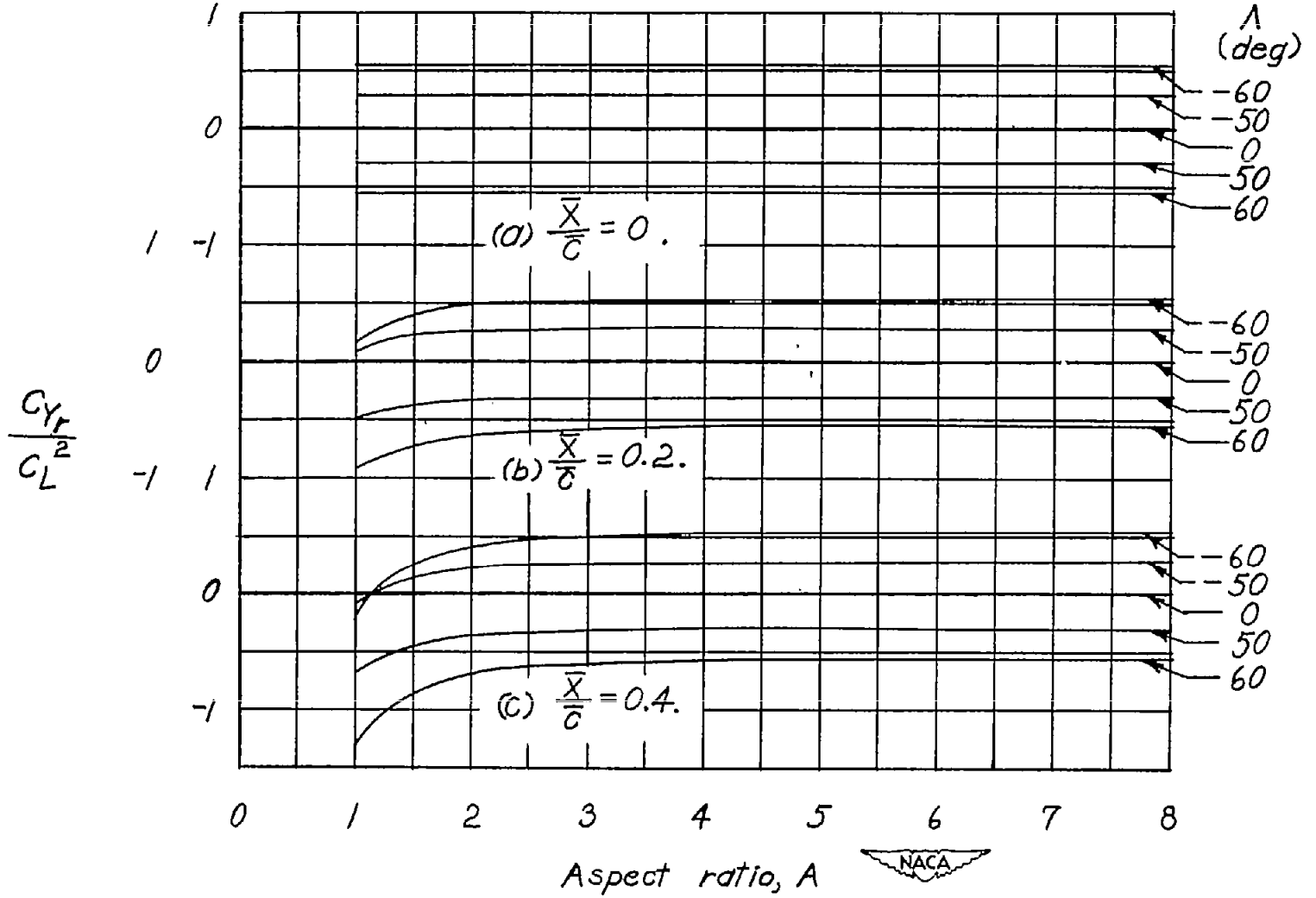

Figure 12.- Chart showing approximate values for the lateral force due to yawing given by equation (39). $\lambda \approx 1.0$.

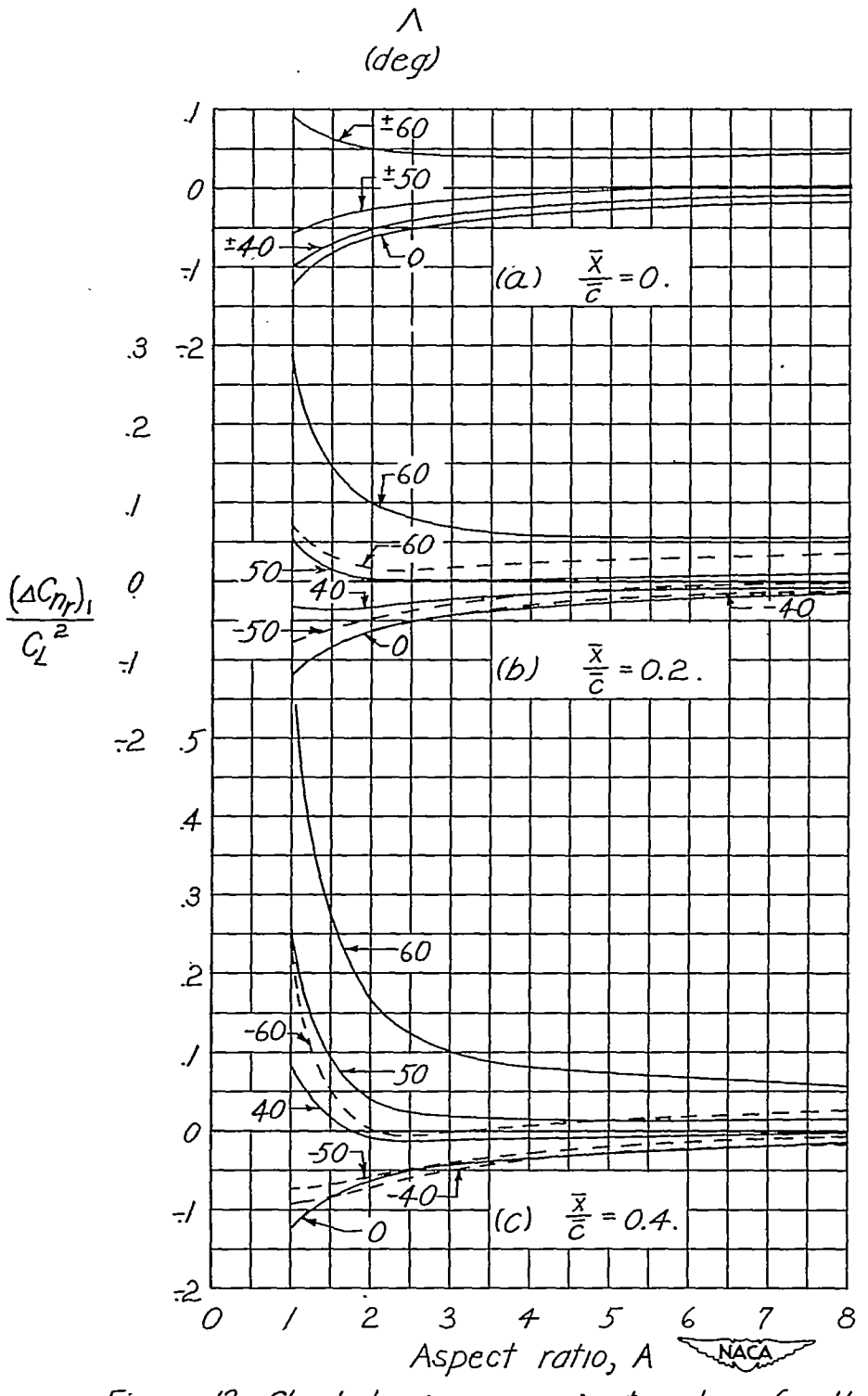

Figure 13.- Chart showing approximate values for the yawing moment due to yawing given by equation (41). Effect of profile drag neglected; $a_o = 5.67$; $\lambda = 1.0$.

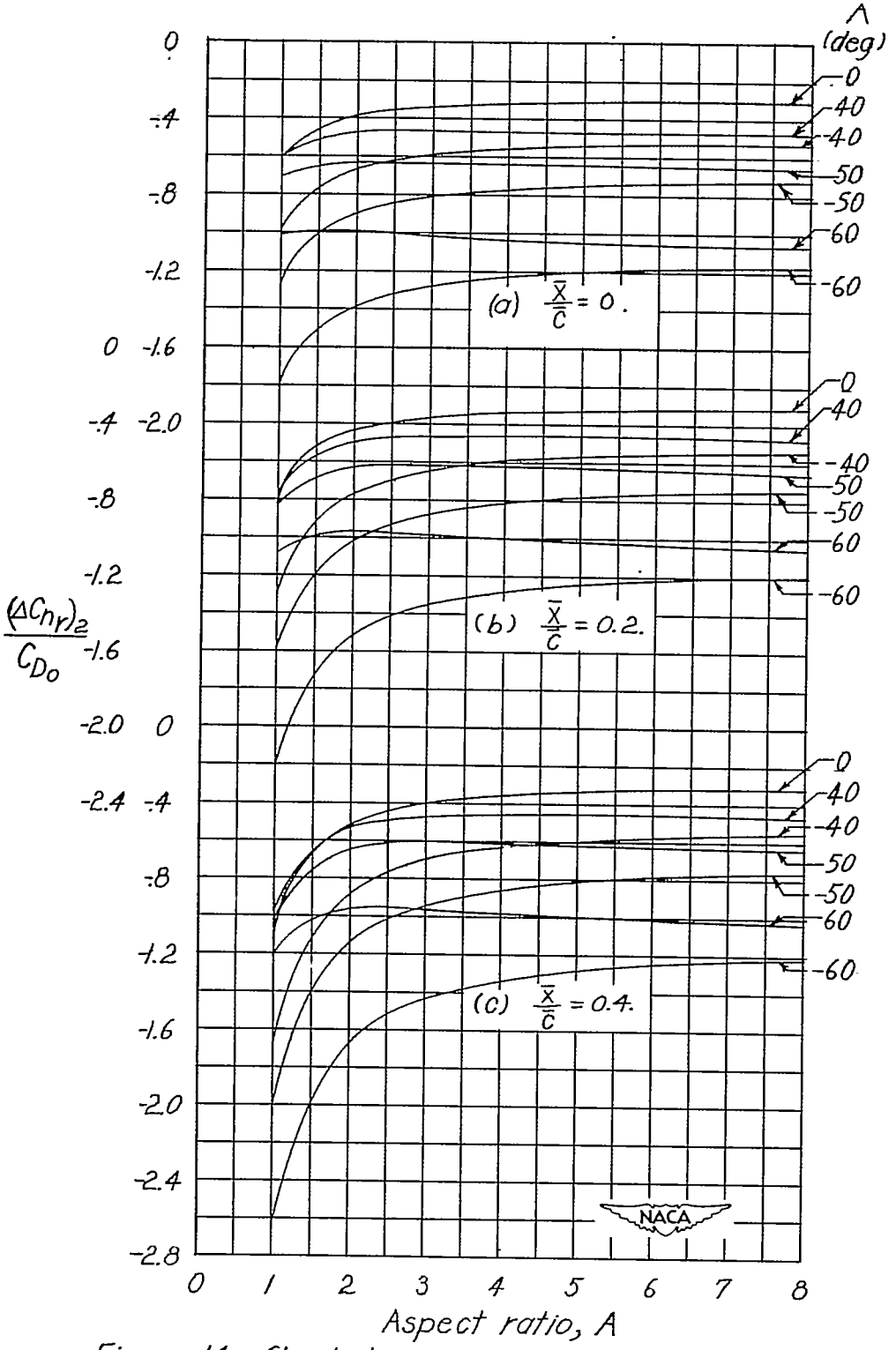

Figure 14.- Chart showing approximate values for the increment of yawing moment due to yawing resulting from profile drag. $\lambda = 0.5$ to 1.0.

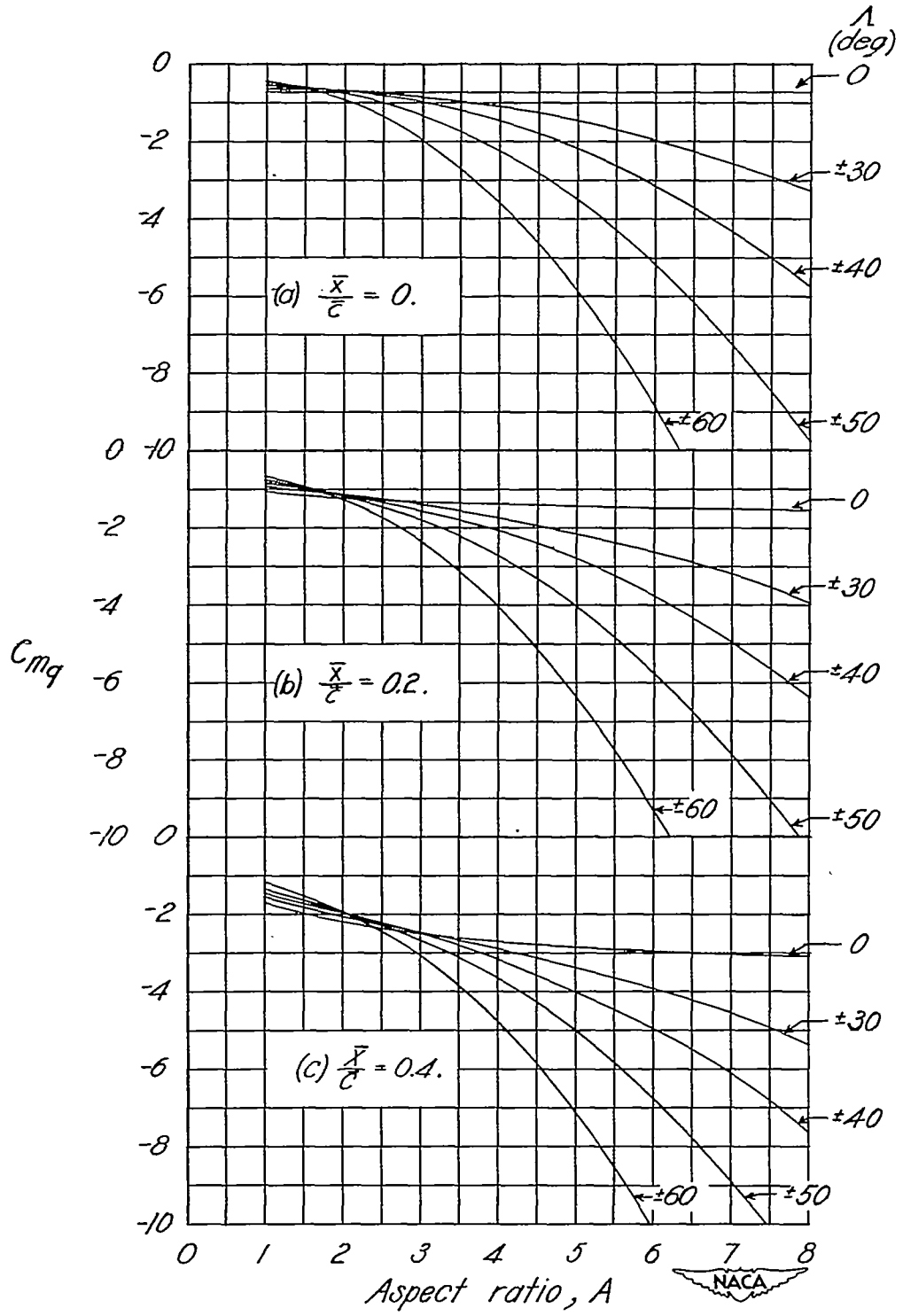

Figure 15.- Chart showing approximate values for the pitching moment due to pitching given by equation (50). $a_0 = 5.67$; $\lambda \approx 1.0$.

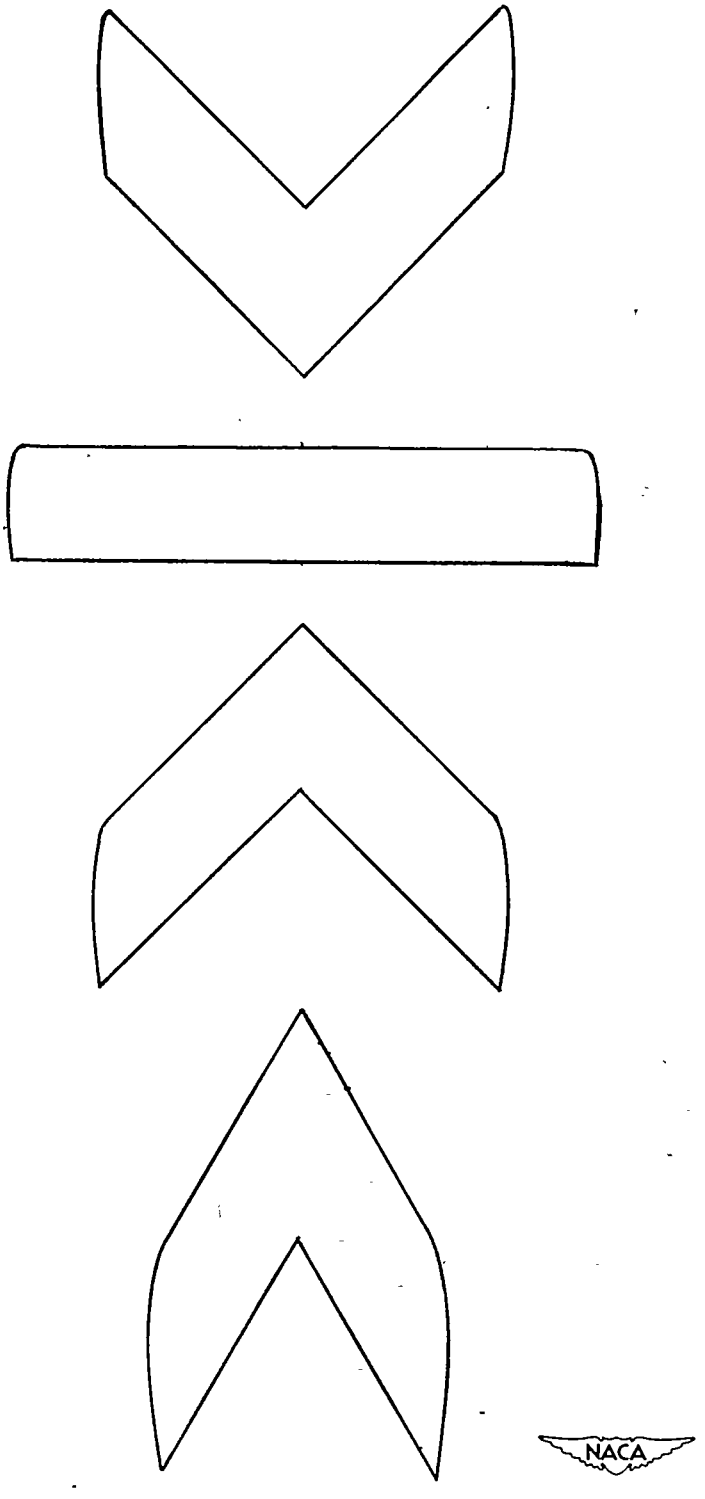

Figure 16.- Series of swept wings investigated in Langley stability tunnel. $\lambda = 1.0$; NACA 0012 airfoil section in planes normal to leading edge.

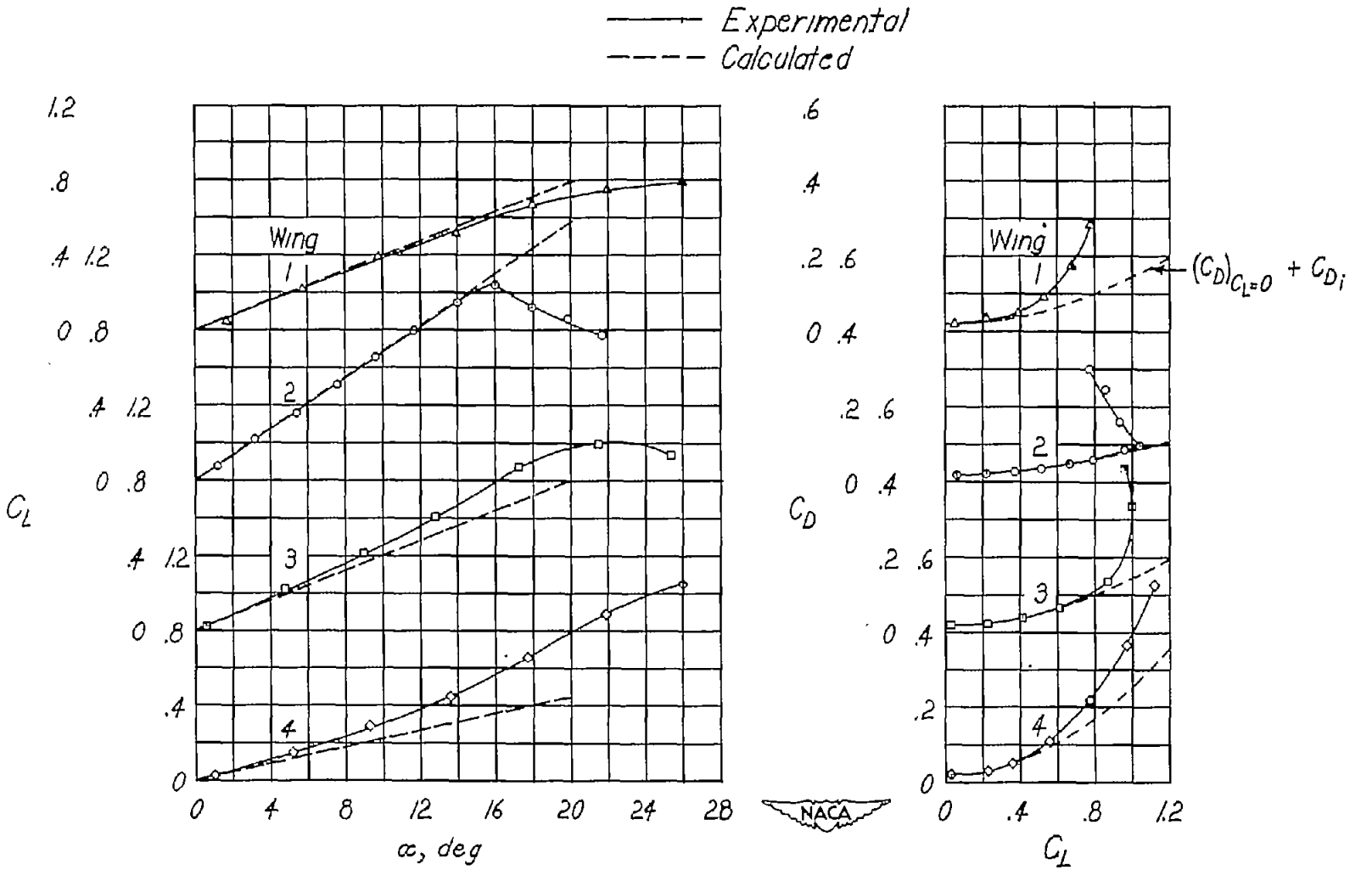

Figure 17.- Comparison of experimental and calculated values for the lift and drag characteristics of the series of swept wings shown in figure 16.

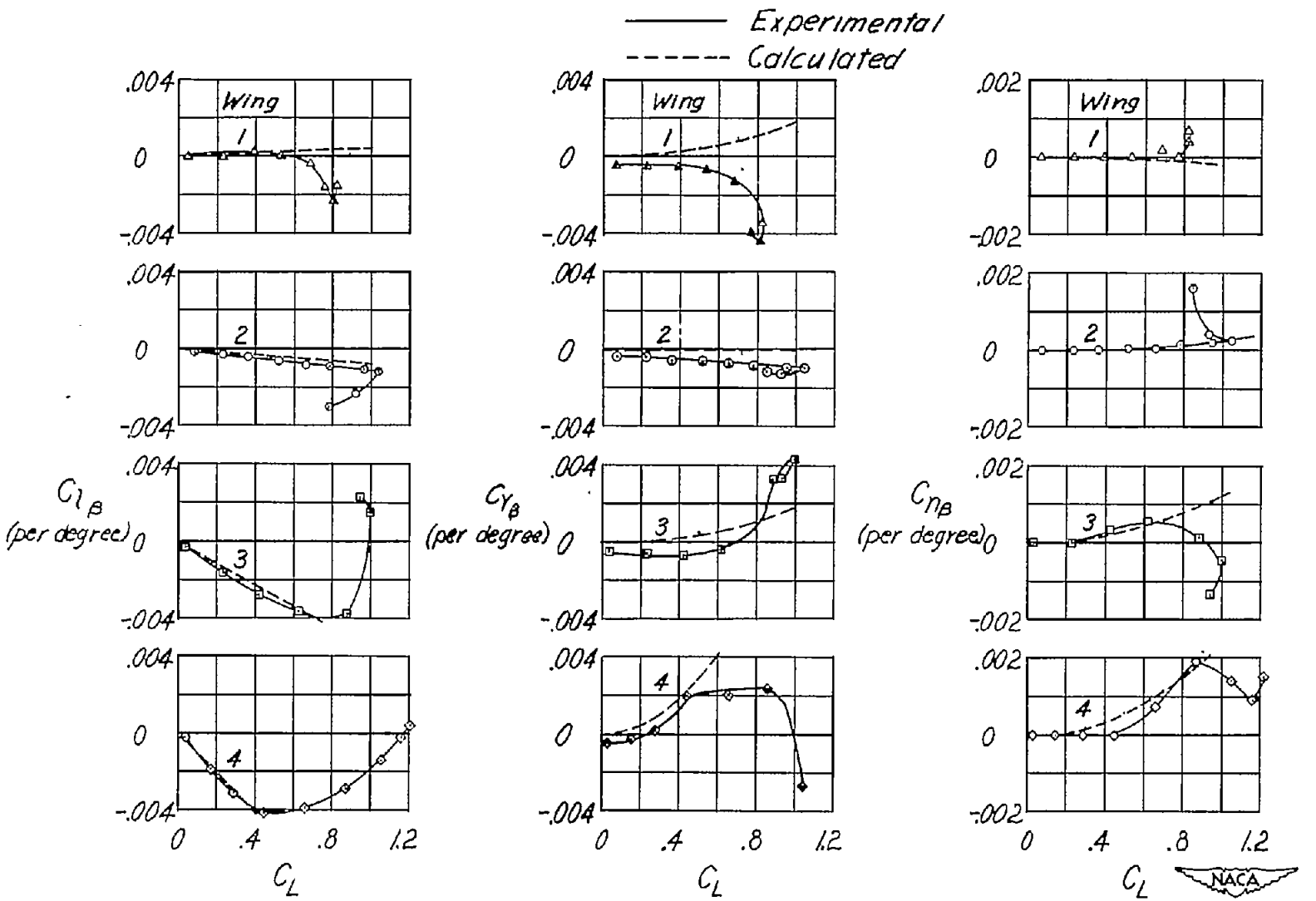

Figure 18.- Comparison of experimental and calculated values for the derivatives in sideslip of the series of swept wings shown in figure 16.

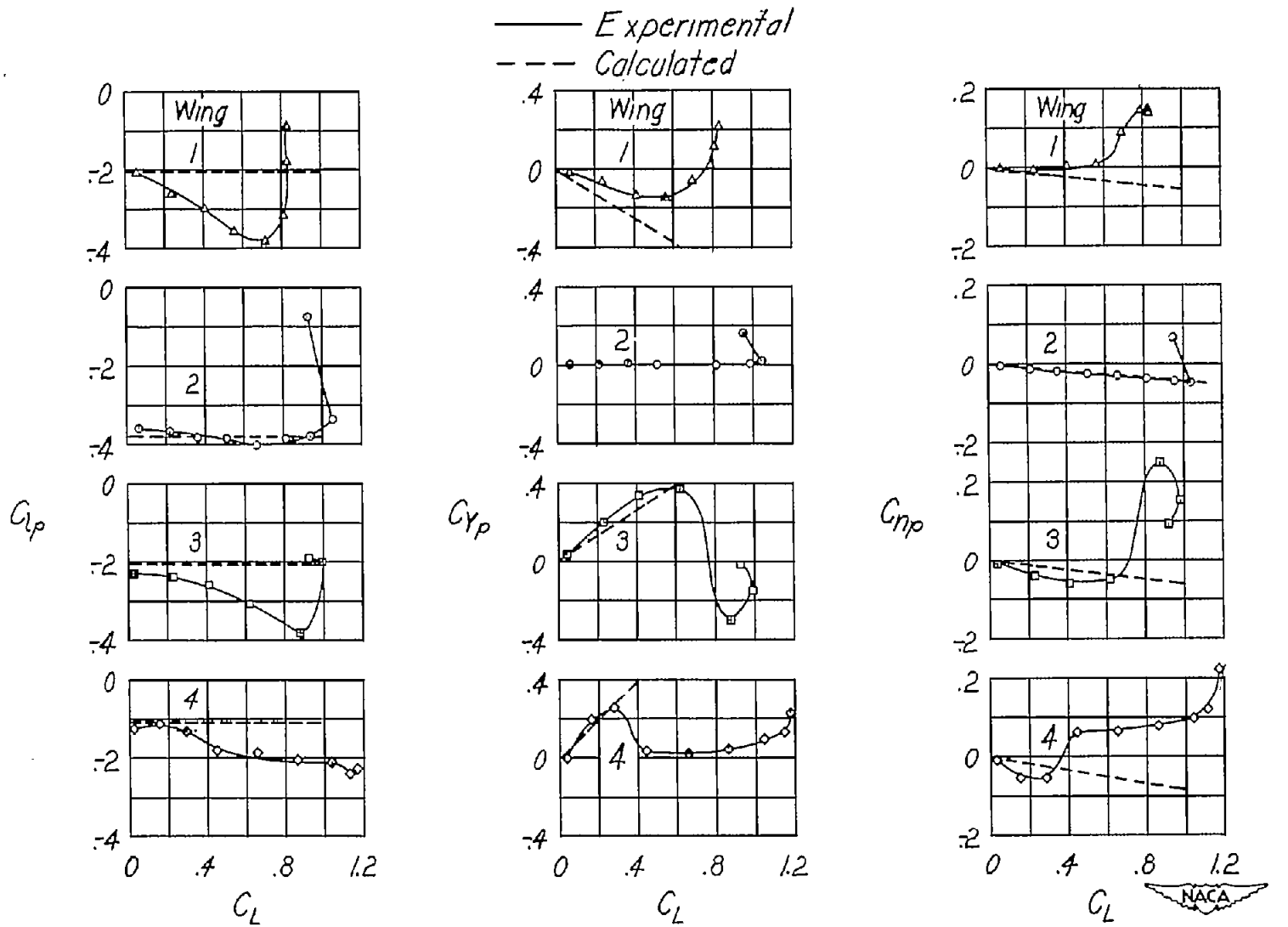

Figure 19.- Comparison of experimental and calculated values for the rolling derivatives of the series of swept wings shown in figure 16.

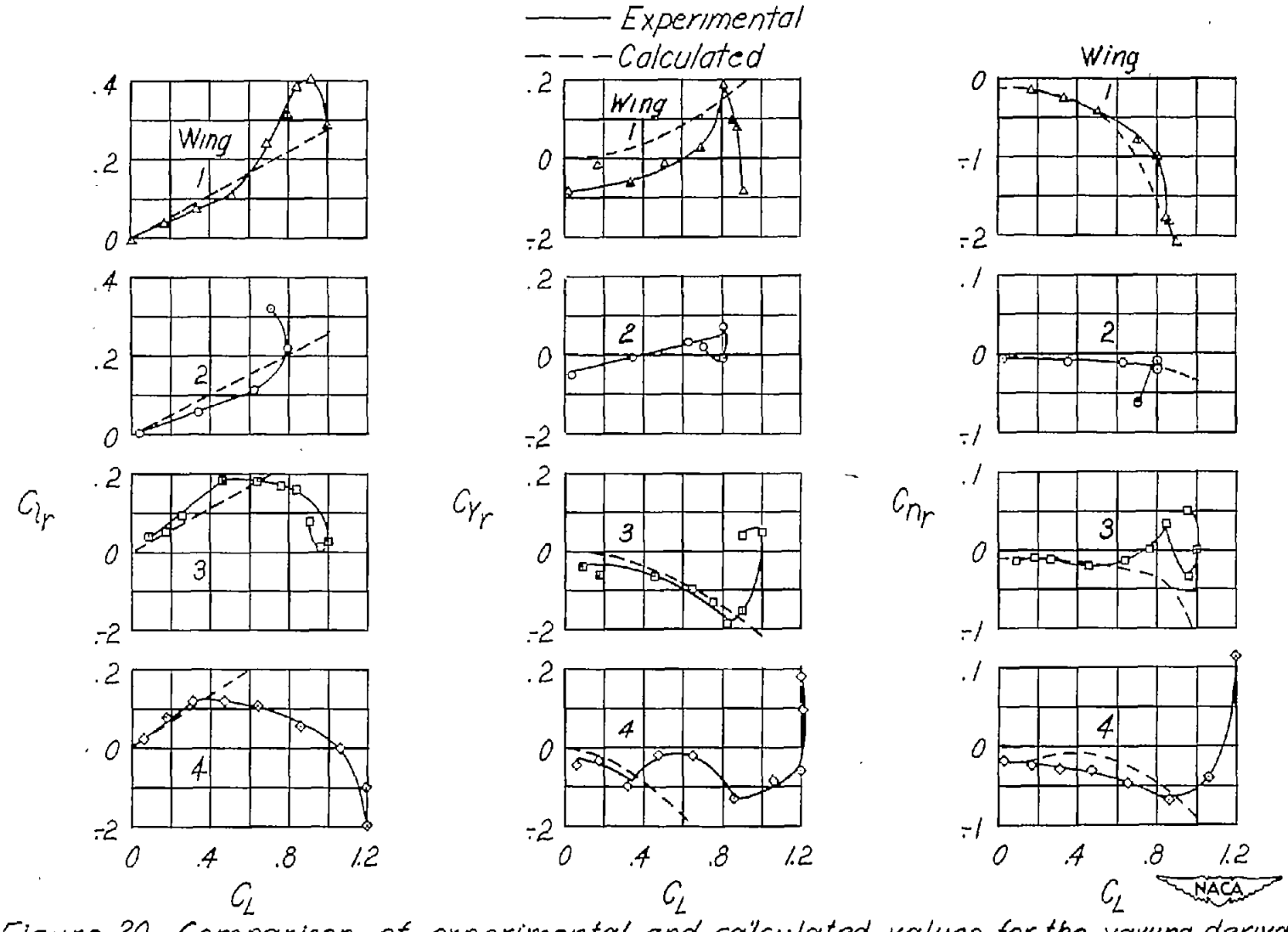

Figure 20.- Comparison of experimental and calculated values for the yawing derivatives of the series of swept wings shown in figure 16.

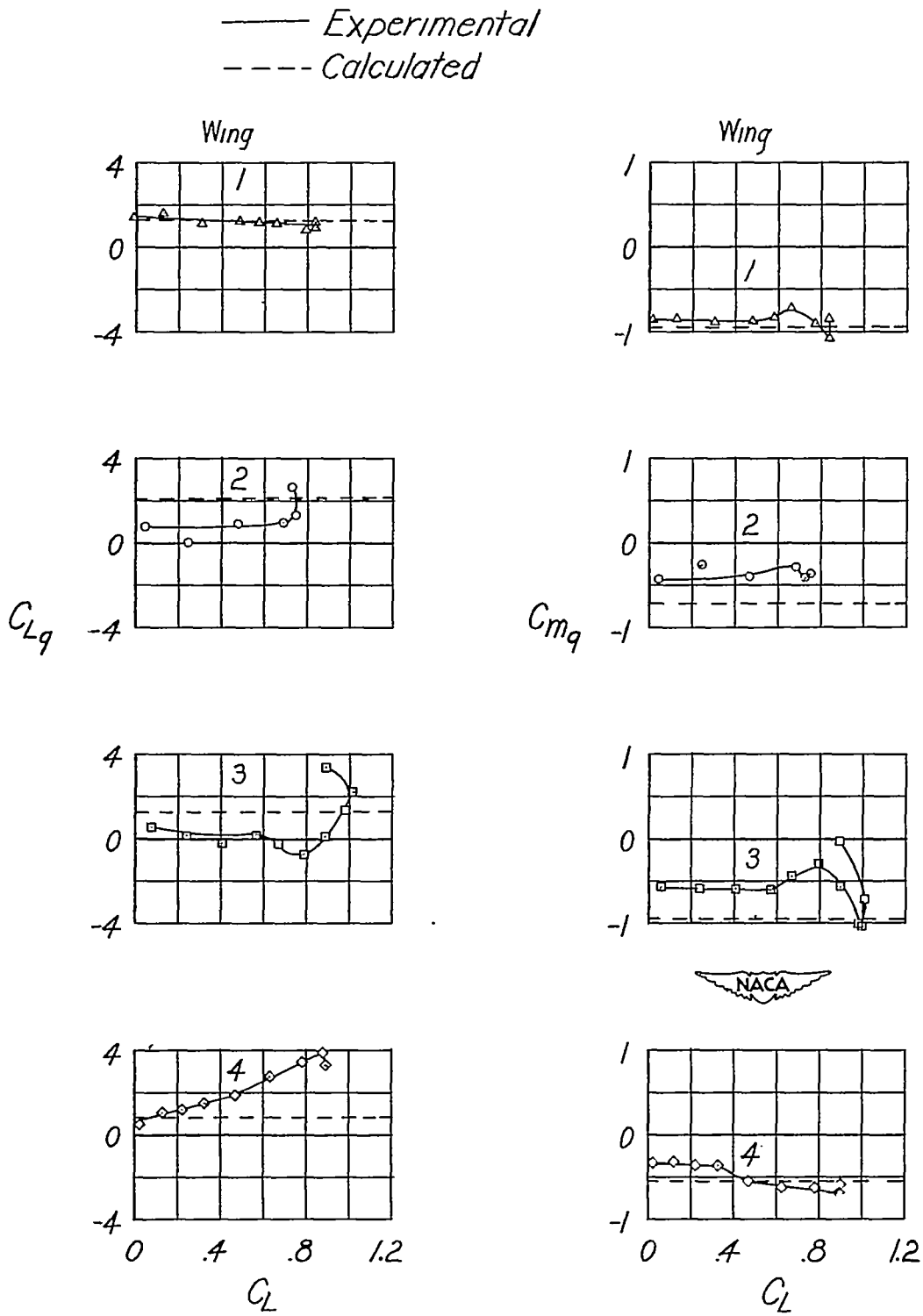

Figure 21.- Comparison of experimental and calculated values for the pitching derivatives of the series of swept wings shown in figure 16.

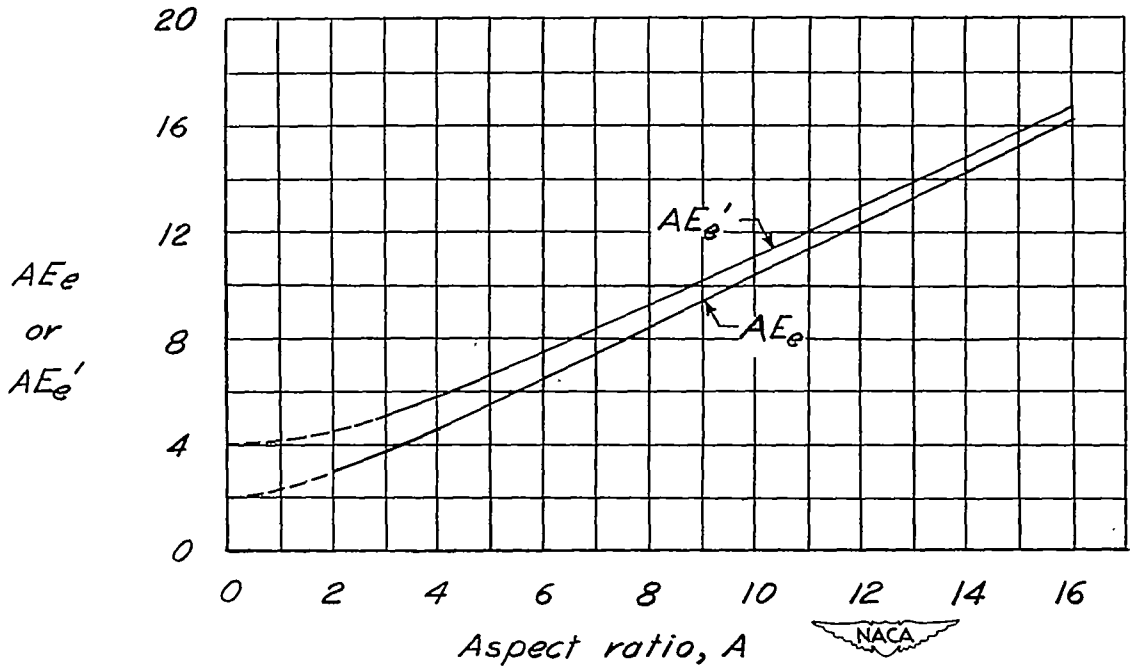

Figure 22.- Curves showing values of the product AE_e and of the product AE_e'.

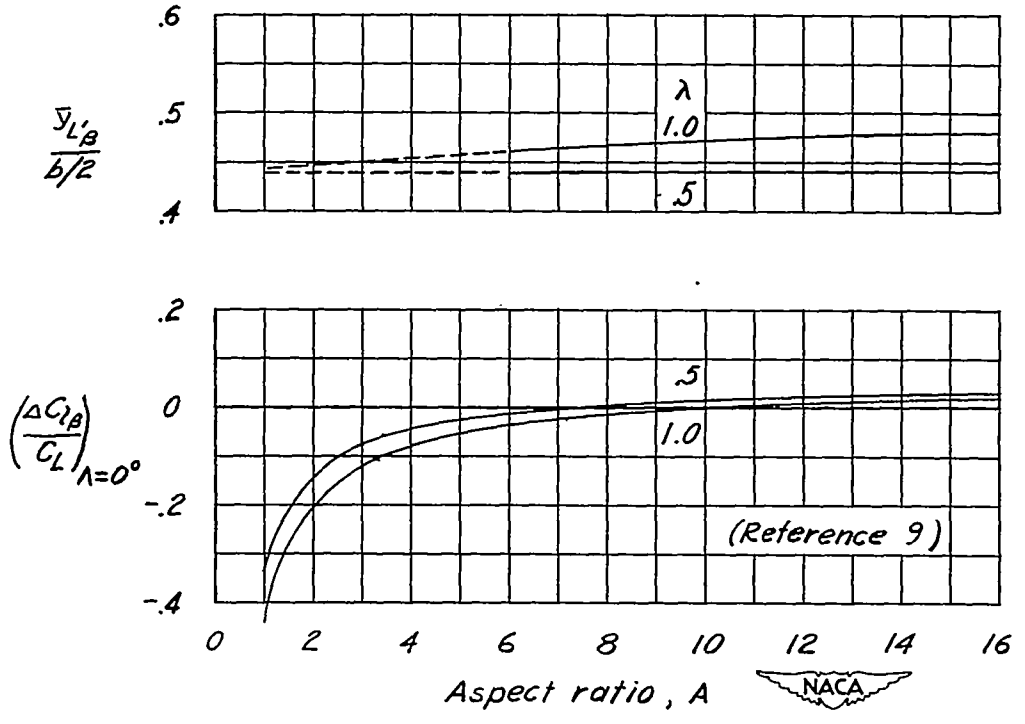

Figure 23.- Extrapolated curves of the effective lateral center of pressure for rolling moment due to sideslip and curves of the increment of rolling moment due to sideslip for unswept wings.

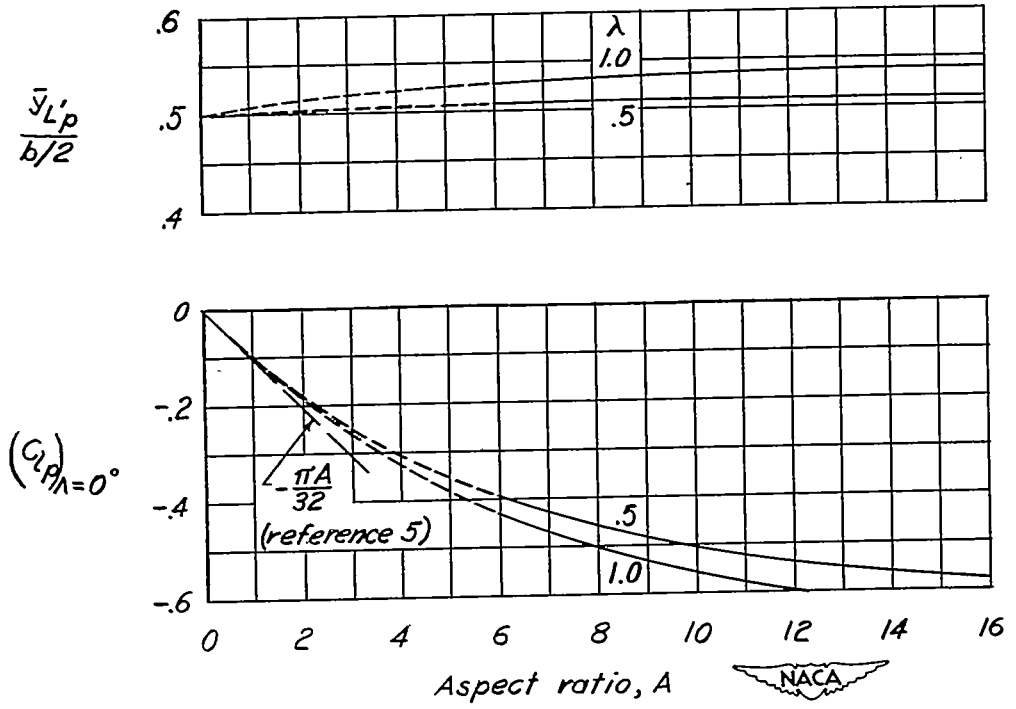

Figure 24.- Extended curves of the effective lateral center of pressure for rolling moment due to rolling and of the derivative of rolling moment due to rolling for unswept wings. $a_o = 5.67$.

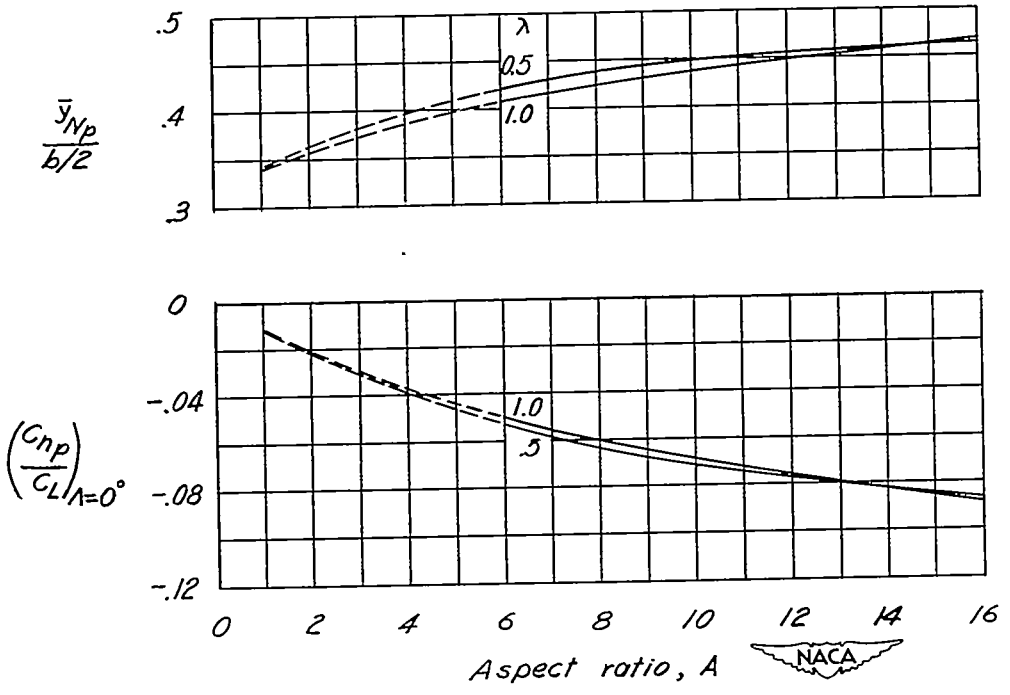

Figure 25.- Extrapolated curves of effective lateral center of pressure for yawing moment due to rolling and of the derivative of yawing moment due to rolling for unswept wings. $a_o = 5.67$.

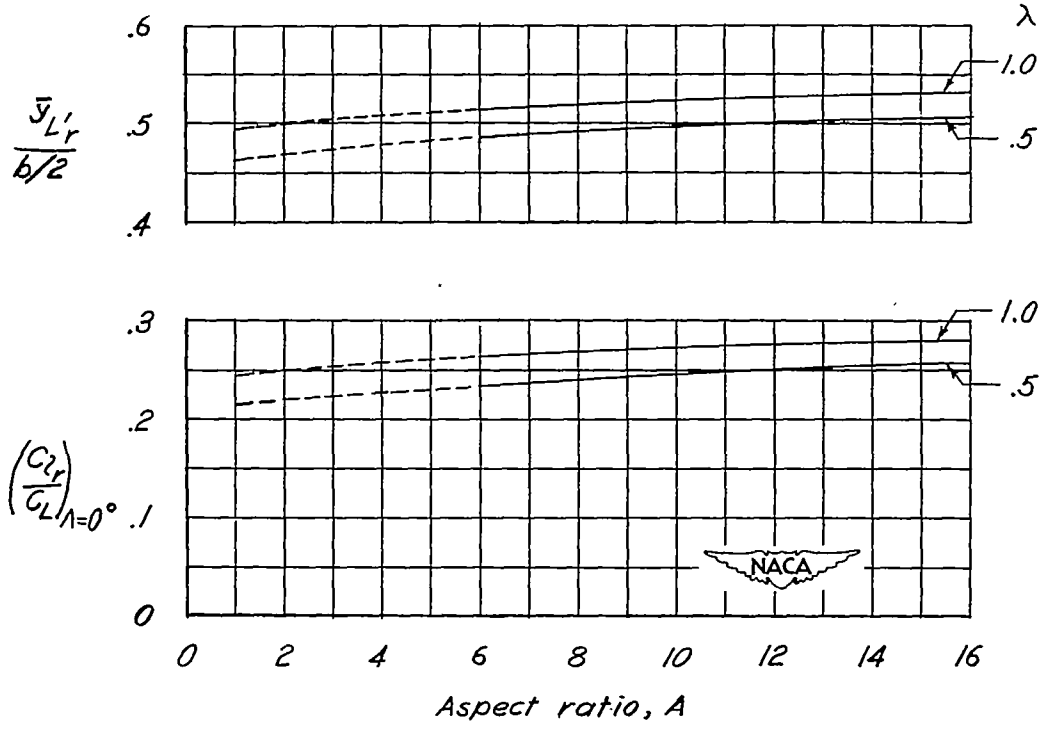

Figure 26.- Extrapolated curves of effective lateral center of pressure for rolling moment due to yawing and of the derivative of rolling moment due to yawing for unswept wings. $a_0 = 5.67$.

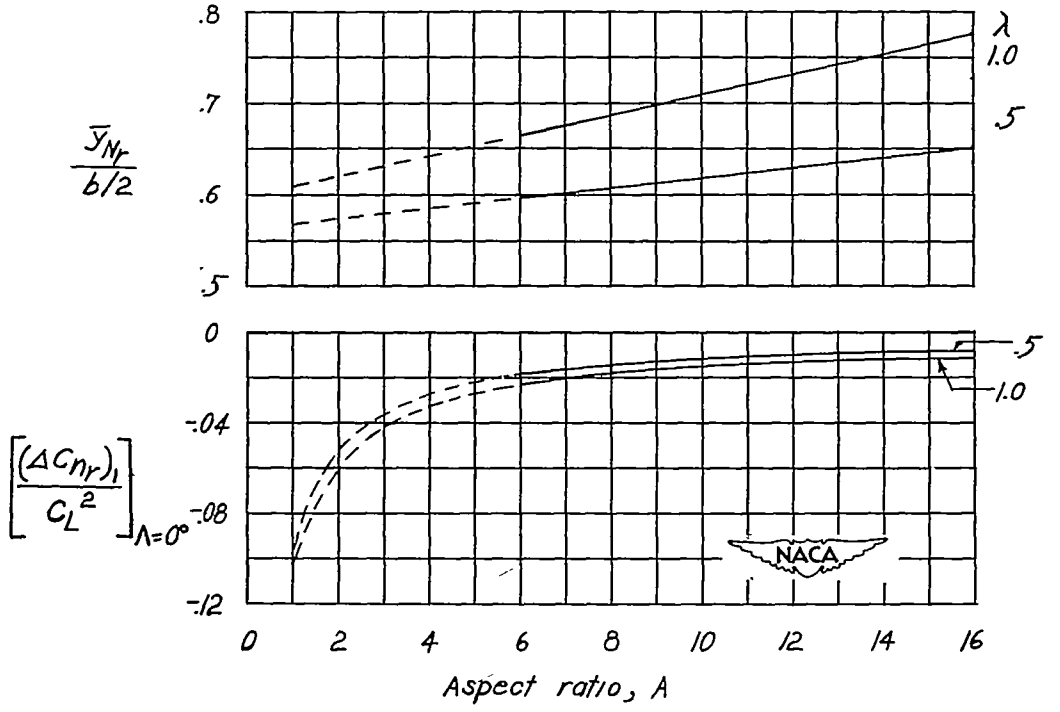

Figure 27.- Extrapolated curves of effective lateral center of pressure for yawing moment due to yawing and of the derivative of yawing moment due to yawing for unswept wings. $a_0 = 5.67$.